Targeting Connexin43 provides anti-inflammatory effects after intracerebral hemorrhage injury by regulating YAP signaling

Hailong Yu
 Nanjing University

Xiang Cao
 Nanjing University

Wei Li
 Yangzhou University

Pinyi Liu
 Nanjing Tech University

Yuanyuan Zhao
 Yangzhou University

Lilong Song
 Yangzhou University

Jian Chen
 Nanjing University

Beilei Chen
 Yangzhou University

Wenkui Yu
 Nanjing University

Yun Xu（✉ xuyun20042001@aliyun.com ）
 Nanjing University Medical School Affiliated Nanjing Drum Tower Hospital   https://orcid.org/0000-0001-5288-0319

Abstract

Background: In the central nervous system(CNS),Connexin43 (Cx43) is mainly expressed in astrocytes and regulates astrocytic network homeostasis. Like Cx43 overexpression,abnormal excessive opening of Cx43 hemichannels (Cx43Hcs) on reactive astrocytes aggravates the inflammatory response and cell death in CNS pathologies.However, the role of excessive Cx43Hc opening in intracerebral hemorrhage (ICH) injury is not clear.

Methods: Hemin stimulation in primary cells and collagenase IV injection in C57BL/6J (B6) mice were used as ICH modals in vitro and vivo.Cx43 mimetic peptide Gap19 was treated after ICH injury. Ethidium bromide (EtBr) uptake assays was used to measure the opening of Hcs. Western blot and immunofluorescence were used to measure the expression of protein. qRT-PCR and ELISA were used to determine the level of cytokines. Co-immunoprecipitation(Co-IP) and Duolink in situ proximity ligation assay (PLA) were applied to measure the association between proteins.

Results: In this study,Cx43 expression was upregulated, and excessive Cx43Hc opening was observed in mice after ICH injury. Delayed treatment with Gap19significantly alleviated hematoma volume and neurological deficits after ICH injury. In addition,Gap19 decreased inflammatory cytokine levels in the tissue surrounding the hematoma and decreased reactive astrogliosis after ICH injury in vitro and in vivo, as determined by GFAP staining. Intriguingly, Cx43 transcriptional activity and expression in astrocytes were significantly increased after hemin stimulation in culture.However,Gap19 treatment downregulated astrocytic Cx43 expression through the ubiquitin-proteasome pathway without affecting Cx43 transcription. Additionally, our data showed that Gap19 increased YAP nuclear translocation, which upregulated SOCS1 and SOCS3 expression, and then inhibited the TLR4-NFκB and JAK2-STAT3 pathways in hemin-stimulated astrocytes. Finally, the YAP inhibitor verteporfin (VP) reversed the anti-inflammatory effect of Gap19 in vitro and almost completely blocked its protective effects in vivo after ICH injury.

Conclusions: This study provides new insight into potential treatment strategies for ICH injury involving astroglial Cx43 and Cx43Hcs.Suppression of abnormal astroglial Cx43 expression and Cx43Hc opening by Gap19 plays anti-inflammatory and neuroprotective roles after ICH injury.

Background

Intracerebral hemorrhage (ICH) refers to the spontaneous rupture of blood vessels in the brain and leads to high morbidity, disability and mortality[1]. The formation of a large hematoma that compresses the surrounding brain tissue results in hematoma compression, which causes neurological deterioration, intracranial hypertension and intracerebral hernia[2]. At the same time, various endogenous molecules are released into the brain parenchyma, which results in cytotoxicity and excitotoxicity through various mechanisms, including neuroinflammation, exacerbation of oxidative stress, and disruption of cell signaling pathways, leading to secondary brain damage during ICH[3].During ICH injury, astrocytes can be

activated by hematoma degradation products, such as hemin chloride. These activates astrocytes accumulate in the area around the hematoma can produce and release cytokinesand chemokines, which aggravate inflammatory responses. Recent studies have reported that inflammatory responses caused by reactive astrocytes play a key role in blood-brain barrier (BBB) destruction and neuronal apoptosis during ICH[4].

Under physiological or pathological conditions, astrocytes maintain communication with the neural microenvironment, mainly through gap junction channels (GJCs). GJCs consist of two juxtaposed half channels (hemichannels, Hcs) between adjacent cells. Hcs are mainly involved in the exchange of ions and small molecules between the intracellular and extracellular environments[5].Physiologically, Hcs are in the off state.However, under pathological conditions such as stroke, excessive opening of Hcs leads to the release of inflammatory factors, glutamate and ATP[6, 7]. Connexin proteins are the basic unit of Hcs. Thus far, eleven types of connexin proteins have been identified in the central nervous system(CNS), and Connexin 43 (Cx43) is the main gap junction protein in astrocytes[8]. Previous studies have shown that like Cx43 overexpression, excessive opening of Cx43 hemichannels (Cx43Hcs) on the surface of reactive astrocytes results in the release of inflammatory factors that aggravate the inflammatory response of the local environment and recruit immune cells to the damaged area under pathological conditions[9, 10].Our previous studies confirmed that astrocytic Cx43 overexpression and excessive Cx43Hc opening aggravates apoptosis and inflammation after cerebral ischemic injury[11, 12].Hence,these pathological processes are reversed by Cx43 mimetic peptides, including Gap26, Gap27 and Gap19, which are short nucleic acid sequences that are derived from the loop of Cx43 and possess the ability to selectively block Cx43Hcs in the CNS[13]. Moreover,Gap19 exerts more protective effects after cerebral ischemic injury than Gap26 or Gap27[12].The reason for this phenomenon may be that Gap19 is more selective in inhibiting Cx43Hcs than Gap26 and Gap27 but does not influence Cx43GJCs, which seems to be beneficial in CNS diseases[14].Intriguingly,linking a TAT membrane translocation motif to the Gap19 N-terminus significantly increases the ability of Gap19 to cross the BBB[14].Therefore,we employed Gap19 to block Cx43Hc opening in this study. However, there is still a lack of evidence for the roles of Cx43 and Cx43Hcs in ICH injury.

Yes-associated protein(YAP) is the transcriptional coactivator of the Hippo signaling pathway. Inactivation of Hippo signaling enhances the dephosphorylation state of YAP, which improves its nuclear capability, leading to antiproliferative and apoptotic effects under different pathophysiological conditions[15]. Unlike other core proteins of the Hippo signaling pathway, including MSTs,LATS and TAZ,YAP has been suggested to be strictly located in astrocytes and neural stem cells.Specifically, members of the TEAD family, including TEAD1, TEAD2, and TEAD3, are the core transcription factors of YAP in the nucleus and are expressed in astrocytes[16]. YAP,the transcriptional coactivator of Hippo signaling, has largely been studied for its role in the immune response,such as its potential transcriptional regulation of the tumor checkpoint receptor PD-1[17, 18].Recently,YAP was investigated for its ability to inhibit the overactivation of astrocytes, which attenuates inflammation in the CNS.Interestingly,YAP has also been found to be sequestered at cells junctions and mechanically bound to Cx43[19]. In this study, we show that the Cx43 mimetic peptide Gap19 inhibits Cx43 expression at the protein level and excessive

opening of Cx43Hcs on astrocytes in mice after ICH. Furthermore, we show that Gap19 provides neuroprotection and promotes cell survival by inhibiting inflammation-associated regulation of YAP signaling in reactive astrocytes after ICH injury.

Methods

Animals

All adult male C57BL/6J (B6) mice (8-10 weeks, 25-30g) were purchased from the Animal Model Center of Nanjing University. All experimental B6 mice were maintained in an air-conditioned room at 25°C.The animals were reared on a 12-h light/dark cycle and provided sufficient food and water. All experimental procedures were approved by the Animal Ethics Committee of Nanjing University and conducted under the guidance of the National Institutes of Health Laboratory Animal Care and Use Guidelines and the Nanjing University Laboratory Animal Management Regulations. All efforts were made to reduce pain in the animals and to obtain as many results from as few mice as possible.

Mice ICH model and treatment administration

Briefly, the mice were anesthetized with an isoflurane-oxygen mixture during the operation and the animal's body temperature was maintained at 37.0 ± 0.5 °C using a heating blanket. The mice were placed in astereotaxic frame, and the skull was cut to expose the skull until Bregma was clearly visible. A hole was drilled 0.5 mm posterior to Bregma and 2 mm lateral to the left (striatal part). The depth of the microsyringe needle was adjusted to 3.5 mm. A micro-infusion pump was connected to a 10 μL syringe, and 0.6 μL of saline containing 0.075 U collagenase IV (Sigma-Aldrich, MO, USA) was injected into the striatum at a rate of 0.12 μL/min. After the injection was completed, the syringe was left in place for 5 min, and slowly withdrawn at a rate of 1 mm every 3 min to prevent backflow after the injection. Then, the drill hole was sealed with bone wax and the suture skin was sterilized. After the operation, the model mice were allowed to recover on a heating pad at 37 °C and the neurological deficits of the mice were closely observed.

TAT-Gap19(25mg/kg,Tocris,#6227) was first administered via intraperitoneal injection (i.p.) 1 hour after ICH and then administered once a day for 2 consecutive days after modeling.The YAP inhibitor verteporfin(Selleck, #1786) was injected into the lateral ventricle(0.1 mg/kg, injected slowly over 10 min) at the same time points via TAT-Gap19.

Behavioral analysis

On the third day after modeling, the modified neurological severity score (mNSS) scale was assessed, and the balance beam test, forelimb strength test and foot failure test were performed to evaluate the neural function of the mice.All procedures were performed by two independent investigators who were unaware of the experimental groups.

mNSS score：The neurological function score is in the range of 0-18: the normal score is 0, 1 point means that the test cannot be completed or lack of reflex, the higher the score, the more serious the neurological deficit, and the most severe neurological deficit score is 18.

Balance beam experiment：Three days before ICH modeling, mice were trained on balance beam walking skills, and the third day after ICH modeling was completed. Place the mouse on the balance beam and score the neurological function according to the walking state of the mouse. The method is as described above. Use a scoring system of 0-6 to evaluate the behavioral changes of the mouse.

Determination of forelimb strength：The mouse forelimb strength test was conducted to detect the recovery of limb function. After the grip meter is zeroed, place the mouse on the platform, in front of the grip rod, grasp the tail of the mouse, and pull straight back. Animals instinctively grab any object when moving backwards unintentionally to prevent backwards, until the pulling force exceeds their grip. After the animal loses its grip, the grip tester automatically records the maximum tensile force and displays it on the LCD screen. Three consecutive measurements, the instrument automatically records the maximum grip strength.

Foot fault test(FFT)：FFT assessed the ability of mice to place their paws on the grid. The mice were trained 3 days before operation, each training lasted for 5 minutes, at least twice a day (at the same time every day). At the end of the third day of training, the average performance of each mouse was taken as the baseline level. On the third day after ICH, the mice were placed on a horizontal metal grid. Record the total number of left forelimbs falling into the grid in 2 minutes. And the total number of steps on the mouse grid. The data of all experimental groups and control groups were measured and used for statistical analysis.

Cultivation of primary astrocytes and treatment administration

Primary astrocytes were obtained from suckling mice within 24 h after birth. The astrocyte cultures in different situation: (1) the control group, cultured with an equal volume of medium (2) the Gap19 group, cultured with Gap19 (100μM/mL, using the same dosage described above) in an equal volume of culture medium,(3)the VP group, cultured with VP (5μM/mL, using the same dose mentioned above) to the same volume of medium, (4) the hemin group, cultured with hemin (20μM/mL, using the same dose mentioned above) to the same volume of medium.Gap19 and VP were added in medium at the begining of hemin stimulation.The cells were used for protein,RNA extraction or immunofluorescence staining after 12 h hemin stimulation.

Lentivirus infection

A lentiviral vector overexpressing Cx43(Lv-Cx43) and a negative control vector (Lv-con) were purchased from Genechem (Shanghai, China). Astrocytes were cultured and incubated with the lentiviruses. After 24 h, the fresh medium was replaced to remove the excessive transfection complex. After 72 h subculture, the cells were harvested under different experimental conditions and used for subsequent experiments.

Ethidium bromide (EtBr) uptake experiment

EtBr staining can be used to observe the activity of Cx43 hemichannels and the role of Gap19. In vivo, frozen sections were prepared using alternate drying, and then the sections were washed with distilled water and hydrated in PBS. The frozen sections were then incubated with a solution containing 0.01% ErTB for 2min, followed by washing with PBS three times for 10min each. The sections were then fixed with 4% PFA, washed again and observed using a fluorescence microscope. ImageJ software was used to analyze the number of EtBr-positive cells in each field of view. In vitro, different cells (astrocytes, microglia, neurons)were inoculated in 24-well plates and then stimulated with hemin and/or Gap19 on glass slides. The cells were then washed twice with PBS and incubated with 0.01% ErTB solution for 5 min. The cells were washed again with PBS and fixed with 4% PFA, followed by washing. The cells were observed and analyzed using the method described above for the in vivo staining.

Luxol fast blue (LFB)

LFB staining was used to evaluate the hematoma volumes and white matter damage on the third day after ICH.Briefly, 0.1% LFB solution was prepared at 60°C for 2 h or 37°C overnight at a constant temperature in a oven. Meanwhile, the prepared frozen sections were dried in an oven at 37°C for 1 h. The sections were hydrated in a 95% ethanol solution for 1 min, placed in the preheated 0.1% LFB solution for 2 h, and then cooled for 30 min. The sections were rinsed in 0.03% lithium carbonate solution and 70% ethanol solution for 2min each. The above steps were repeated until the difference between the gray matter and white matter was obvious. Then, the sections were dehydrated in an ethanol solution for 2min, and then sealed with transparent xylene and neutral gum. Damage to the myelin sheath of the white matter after cerebral hemorrhage was analyzed by fluorescence microscopy and ImageJ software.

Fluoro-Jade C (FJC) staining

Prepared frozen sections were dried at room temperature (RT), hydrated with distilled water for 2min, immersed in an 80% ethanol solution containing 1% NaOH for 5min, and then washed in a 70% ethanol solution, followed by distilled water for 2min each. The sections were then incubated in 0.06% potassium permanganate for 10min, washed and reacted in a 0.0001% fluoro jade prepared with 0.1% acetic acid C working solution for 10min. After the sections were washed again, they were dried, and then sealed with transparent xylene and neutral gum.The apoptotic neurons in the brain tissue around the hemorrhage were observed under a fluorescence microscope.

Immunofluorescence

The method described above was used to prepare frozen sections on the third day after ICH in model mice or inoculated astrocytes, microglia and neurons on slides for immunofluorescence staining. After treatment, sections or cells were incubated overnight with antibodies against GFAP(1:200, Cell Signaling Technology, #80788), Iba1(1:100, Cell Signaling Technology, #17198), Nuen(1:50, Cell Signaling Technology, #24307), or YAP(1:100, Cell Signaling Technology, #14074). After washing, the sections or

cells were incubated for 2 h with the indicated secondary antibodies (Invitrogen, 1:500) in the dark at R). After washing in PBS, the samples were stained with 4',6-diamino-2-phenylindole (DAPI) to label the nuclei. All staining results were observed using a fluorescence microscope.

Nuclear/cytoplasmic protein separation and extraction

Nuclear and cytosolic proteins were extracted using a nucleocytoplasmic separation and extraction kit (Thermo-Fisher Scientific,MA,USA) as previously described (PMID: 27998743). The supernatants were collected and the protein concentrations were measured using the BCA method(Thermo-Fisher).

Co-immunoprecipitation

After extraction and treatment, different groups of astrocyte proteins were subjected to a co-immunoprecipitation assay. Briefly, astrocytes were inoculated into 6-well plates at a density of 6×10^5, cultured for 24 h under suitable conditions, treated for 24 h with different experimental conditions, and then split and homogenized in immunoprecipitation lysis buffer. The immunoprecipitation samples were collected and incubated with anti-YAP(1:50, Cell Signaling Technology, #14074),anti-Cx43 (1:30, Abcam, #235585)or rabbit IgG (1:20, Cell Signaling Technology, #3424)antibodies at 4°C with gentle shaking overnight for co-immunoprecipitation.Then, 10 μL of protein A agarose beads were added to the samples, followed by incubation in a 4°C shaker for an additional 2 h. After centrifugation, the supernatant was carefully removed by suction, and the agarose beads containing the immune complexes were washed 3 times with lysis buffer solution.Finally, sample buffer solution was added and the samples were boiled for 5 min; the supernatant was collected for subsequent Western blot (WB) analysis.

To demonstrate the interaction between Gap19 and Cx43 or YAP, streptavid in magnetic beads (MCE, HY-K0208) were used. Primary astrocytes were preincubated with biotinylated Gap19(Gap19-biotin,100μM/mL,) for 30 min at 4°C.The other procedures were the same as described above.

Duolink in situ proximity ligation assay (PLA)

PLA was performed according to the manufacturer's instructions (Duo92012; Sigma-Aldrich, St. Louis, MO, USA).Briefly, astrocytes were seeded on glass slides, followed by treatment with the above described experimental conditions. The astrocytes were washed, blocked and then incubated with anti-YAP (1:100) or anti-Cx43 (1:100) primary antibodies overnight at 4°C. After washing, the astrocytes were incubated with Duolink PLA probes MINUS and PLUS for 1 h at 37°C. A Duolink in situ detection kit was used for ligation and amplification. DAPI was used to stain the nuclei. The images were captured using a confocal fluorescence scanning microscope, and the red spots indicated the interaction between YAP and Cx43.

Western blot

At 6h, 12h, 24h, 3d, and 7d after ICH, mice were sacrificed and the brains were quickly removed.The brain tissue around the hemorrhage area was collected or different astrocytes were collected after different treatment, as described above. The total protein was extracted using a protein extraction kit, and then the

protein concentration in the supernatant was measured by the BCA method.After quantitative analysis, equal amount of proteins were separated with 10% SDS-PAGE and then transferred to PVDF membranes. After blocking with 5% skim milk at RT for 2 h, the PVDF membranes were incubated with the following primary antibodies: anti-IL-1β(1:1000,Cell Signaling Technology, #12703), anti-IL-4(1:1000, Cell Signaling Technology,#12227), anti-IL-6(1:1000, Cell Signaling Technology, #12912), anti-IL-10(1:1000, Cell Signaling Technology, #12163), anti-MCP-1(1:1000, Cell Signaling Technology, #2027), anti-TNF-α(1:1000, Cell Signaling Technology, #11948), anti-Cx43(1:1000, Cell Signaling Technology, #3512), anti-YAP(1:1000, Cell Signaling Technology, #14074), anti-phospho-YAP(1:1000, Cell Signaling Technology, #13008), anti-SOCS1(1:1000, Cell Signaling Technology, #3950), anti-SOCS3(1:1000, Cell Signaling Technology, #52113), anti-JAK2(1:1000, Cell Signaling Technology, #3230), anti-phospho-JAK2(1:1000, Cell Signaling Technology, #3771), anti-STAT3(1:1000, Cell Signaling Technology, #9139), anti-phospho-STAT3(1:1000, Cell Signaling Technology, #9145), anti-TLR4(1:1000, Cell Signaling Technology, #14358), anti-P65(1:1000, Cell Signaling Technology, #8242), anti-phospho-P65(1:1000, Cell Signaling Technology, #3033), anti-IKBα(1:1000, Abcam, #32518), anti-IKKβ(1:1000, Cell Signaling Technology, #8943), anti-phospho-IKKβ (1:1000, Cell Signaling Technology, #2697), anti-H3(1:1000, Cell Signaling Technology, #4499) and anti-tubulin (1:1000, Cell Signaling Technology, #2128), overnight at 4°C on a shaker. After washing the next day, the membranes were incubated at secondary antibody for 2 h. Subsequently, the enhanced chemiluminescence system (ECL) was used to observe the proteins. The different protein bands were analyzed quantitatively by ImageJ software.

Total RNA extraction and quantitative real-time PCR analysis

Astrocytes were inoculated and cultured for 24 h under suitable conditions, and then treated for the indicated times and experimental conditions as described above. Total RNA was extracted with TRIzol reagent (Invitrogen, CA,USA)and reversed transcribed to cDNA with the PrimeScript RT Reagent Kit (Takara). The expression of IL-1β, IL-6, TNF-α, MCP1 and Cx43 was detected using the SYBR Green Kit (Takara) on a ABI 7500 PCR system. The corresponding primers used were as follows:

Gene	Primer Forward (5′- 3′)	Primer Reverse (5′- 3′)
IL-1β	GTCTGACCCATGTGAGCTG	GCCACAGGGA TTTTGTCGTT
IL-6	TACCCCAACT TCCAATGCTC	GGTTTGCCGA GTAGACCTCA
TNF-α	GGAACACGTCGTGGGATAATG	GGCAGACTTTGGATGCTTCTT
IL-10	TCAAGGATGCACATCAAAAGGC	AGGCAGCAACTTCCTCCCT
MCP1	CTCGGACTGTGATGCCTTAAT	TAAATGCAAGGTGTGGATCCA
Cx43	CTCGCCTATGTCTCCTCCTG	TTTGCTCTGCGCTGTAGTTC
GAPDH	GCCAAGGCTGTGGGCAAGGT	TCTCCAGGCGGCACGTCAGA

Statistical analysis of the data

All data are expressed as the mean ± SEM of at least three independent experiments. T tests were used to compare the means of two groups. One-way ANOVA was used for the comparison of multiple groups. P<0.05 was considered statistically significant, and P<0.01 was considered highly statistically significant.The immunofluorescence images were obtained by a fluorescence microscope and analyzed by ImageJ software. GraphPad prism 7 (CA, USA) was used to draw the statistical charts.

Results

Cx43 overexpression is accompanied by abnormal Cx43Hc opening after ICH injury

At present, there is no definitive conclusion on the expression of Cx43 after ICH injury. In this study, Cx43 expression was measured at different time points after ICH.As shown in Figure 1A and B, Cx43 expression was upregulated in the ICH group compared to the sham group beginning 6 h after ICH injury, peaked at 72 h after ICH injury and became retuned at 96 h after ICH injury (P<0.05). Previous studies have revealed that under pathological conditions, Cx43overexpression is accompanied by abnormal excessive opening of Cx43Hcs[10]. EtBr analysis was employed to detect the opening of Hcs in our study.The activity of Hcs was significantly increased in the ICH groups compared with the sham group.Interestingly,consistent with the protein level of Cx43, the opening of Hcs gradually increased and peaked 72 h after ICH injury(P<0.01, Figure 1C,D). These results indicate that Cx43 and Cx43Hcs may play important roles in the pathological process after ICH injury.According to the above results,we chose72 h after ICH as the observation time point for the subsequent studies.

TheCx43 mimetic peptide Gap19provides neuroprotection after ICH injury

The Cx43 mimetic peptide Gap19 is used as a selective blocker of Cx43Hcs in the CNS under pathological conditions[20, 21]. Our previous research revealed that Gap19 provides protective effects against cerebral ischemic stroke by reducing infarct volume and alleviating neurological deficits[11, 12]. In this study, we examined its role in the pathological process of ICH injury. The excessive opening of Cx43Hcs was significantly reduced in the TAT-Gap19-treatedICH group compared to the ICH group (P<0.01, Figure 2A, B). The number of apoptotic neurocytes was also significantly decreased in the TAT-Gap19-treated ICH group compared to the ICH group (P<0.05, Figure 2C, D). LFB stainingcan be used to detect white matter damage and to evaluate the hematoma volume after ICH.We stained mouse brain sections and measured the surviving blue-stained area 72h after ICH.The results showed that compared to vehicle treatment, TAT-Gap19 treatment significantly reduced the hematoma volume.The blue-stained area of mouse brain sections from the TAT-Gap19 + ICH group was much larger than that of mouse brain sections from the ICH group (71.72 ± 5.719 vs 51.2 ± 3.507%, P<0.01, Figure 2E, F).

Gap19 improves neurological dysfunction after ICH injury

Considering the obvious protective effects of Gap19 treatment in reducing hematoma volume and apoptosis after ICH injury, we further detected the effect of Gap19 on neural function. Three days after

continuous intraperitoneal injection of TAT-Gap19, behavioral tests including the balance beam experiment,forelimb strength test and foot fault test were performed, and mNSSs were assigned.

Our data showed that TAT-Gap19 treatment did not influence mouse neurobehavioral function under physiological conditions (P>0.05, Figure G-J), which is consistent with our previous studies[11, 12]. The mNSSs of the mice were significantly increased by ICH damage, while TAT-Gap19 treatment markedly reduced mNSSs (11.20 ± 1.30 vs 6.50 ± 1.29, P<0.01, Figure 2G). The balance beam experiment reflects muscle strength and extremity balance. The results showed that the scores of the TAT-Gap19 + ICH group were significantly lower than those of the ICH group (2.6 ± 0.55 vs 6.00 ± 0.82, P<0.01, Figure 2H). Then, the forelimb strength of the mice was measured.The grip strength of the ICH group (92.58 ± 9.497 g) was significantly lower than that of the TAT-Gap19 + ICH group (123.6 ± 6.328 g, P<0.05, Figure 2I). Finally, we detected the foot fault rates of the mice after ICH to evaluate the ability of the mice to integrate and coordinate movement. Compared with that of the sham group, the foot fault rate of the ICH group was significantly increased, and the TAT-Gap19 + ICH group exhibited a significantly lower foot fault rate than the ICH group (48.00 ± 9.80% vs 24.00 ± 3.58%, P<0.01, Figure 2J). These findings confirm that Gap19 exerts an obvious neuroprotective effect in mice after ICH injury.

Gap19 reduces proinflammatory cytokines in vivo after ICH injury

Inflammation is considered to be the core factor underlying secondary damage after ICH injury.Various proinflammatory cytokines and chemokines, including IL-6, IL-1β, TNF-α and MCP-1, which aggravate tissue injury, are produced and secreted into the brain parenchyma[22].However, anti-inflammatory cytokines such as IL-4 and IL-10 can also be released by immune cells after ICH-induced damage[23].In a previous study, blocking Cx43Hcs with a Cx43 mimetic peptide was demonstrated to inhibit inflammation[24].In this study, we used WB to evaluate the expression levels of proinflammatory cytokines, including IL-1β, IL-6, TNF-α, and MCP-1, and anti-inflammatory cytokines, including IL-4 and IL-10, 72 h after ICH. After ICH injury, the levels of IL-1β, IL-6, TNF-α and MCP-1 were markedly upregulated.Intriguingly, compared to the ICH group, TAT-Gap19 not only decreased the expression levels of proinflammatory cytokines (IL-1β, IL-6, TNF-α and MCP1) but also increased the levels of anti-inflammatory cytokines (IL -4 and IL-10) after ICH injury (P<0.05, Figure 3A-D).

Gap19 reduces astrocyte activation and astrocytic proinflammatory cytokine production after ICH injury

Because Cx43 is most abundant in astrocytes and regulates the network between other cells in the CNS through gap junctions, we measured the pharmacological effects of Gap19 in blocking the activity of Hcs on different types of primary neurocytes, including astrocytes, microglia and neurons, after 12 h of hemin stimulation.In culture, EtBr uptake by all three types of neurocytes was higher in the hemin-treated groups than that in the control groups (P<0.01, Figure 3E, F).Interestingly,after hemin stimulation, Gap19 slightly blocked the opening of Hcs on neurons and microglia, but the difference was not significant (P>0.05, Figure 3E, F).However, compared to vehicle, Gap19 significantly inhibited the opening of astrocytic Hcs after hemin stimulation (P<0.01, Figure 3E, F). Based on these results, we explored whether abnormal Cx43Hc opening mainly occurs on the surface of astrocytes after ICH injury.

A previous study reported that Cx43 may be related to the activation of astrocytes and that Cx43 peptides can reduce the number of reactive astrocytes after ischemic stroke[20]. We labeled reactive astrocytes after ICH injury in vivo and intro by staining for GFAP. In mouse sections from the sham group, a small number of reactive astrocytes was observed in the peripheral area of the striatum;however, there was a significant increase in reactive astrocytes around the cerebral hematoma in the ICH group compared to the sham group 72 h after ICH injury (P<0.01, Figure 3G,H). Compared to no treatment, treatment with TAT-Gap19 markedly reduced the number of reactive astrocytes compared with that in the ICH group (P<0.01, Figure 3G, H). We obtained consistent results in astrocytes subjected to hemin stimulation, which was used to simulate ICH injury in vitro. Compared to no treatment, Gap19 treatment significantly reduced the GFAP fluorescence intensity, which was much higher in the astrocytes stimulated with hemin for 12 h than in unstimulated astrocytes (P<0.01, Figure 3I, J). These results indicate that blocking astrocytic Cx43Hcs with Gap19 can reduce the number of reactive astrocytes after ICH injury.

Studies have shown that reactive astrocytes produce and release various proinflammatory cytokines and chemokines after brain injury[25].In this study,the transcriptional activity of proinflammatory cytokines and chemokines, including IL-1β, IL-6, TNF-α and MCP-1, in cultured astrocytes was measured by qRT-PCR 12 h after hemin stimulation.The transcriptional activities of IL-1β, IL-6, TNF-α and MCP-1 were upregulated after hemin stimulation. In the hemin group, compared to no treatment, Gap19 markedly alleviated the transcriptional activity of upstream proinflammatory cytokines and chemokines (P<0.01, Figure 4A). Furthermore, ELISA was employed to evaluate proinflammatory cytokine and chemokine release by cultured astrocytes after hemin stimulation. Much higher levels of IL-1β, IL-6, TNF-α and MCP-1 were detected in the supernatants of the hemin group than in the supernatants of the control group.However, compared to no treatment, Gap19 reduced the secretion of upstream proinflammatory cytokines and chemokines by astrocytes after hemin stimulation (P<0.05, Figure 4, B-E). These findings further demonstrate that Gap19 exerts protective effects against ICH-induced inflammation.

Gap19promotes the degradation of astrocyticCx43 through the ubiquitin-proteasome pathway after hemin stimulation

To explore the effects of Gap19 treatment on astrocytic Cx43 after ICH injury, we used WB and qRT-PCR to detect the expression level of astrocytic Cx43 in cultured cells after hemin stimulation. Total protein and RNA were extracted from astrocytes cultured under different conditions. Both the protein level and transcriptional activity of Cx43 were markedly increased in the hemin group compared with control group (P<0.01, Figure 5A-C). At the same time, qRT-PCR analysis further confirmed that compared to no treatment, Gap19 treatment reduced the overexpression of Cx43 induced by hemin stimulation (P<0.01, Figure 5C). However,Gap19 decreased the protein level but not the transcriptional activity of astrocytic Cx43 compared with that in the hemin group. Thus, Gap19 may affect the stability of Cx43 in astrocytes after ICH injury, which is in agreement with the effects of Gap19 on cerebral ischemia injury observed in our prior study[11].

There is sufficient evidence showing that ubiquitination plays a key role in Cx43 degradation, which contributes to functional changes in gap junction channels. Studies have found that Cx43 can be rapidly degraded either by lysosomes or through the ubiquitin-proteasome pathway[26]. To further evaluate the degradation mechanism of astrocytic Cx43 after hemin stimulation, the proteasome inhibitor MG132 and lysosomal inhibitor chloroquine were used. WB analysis showed that MG132 treatment almost reversed the effect of Gap19 on astrocytic Cx43 degradation after hemin treatment (P<0.01), while chloroquine did not have any significant anti-degradation effects (Figure 5D, E). We further detected the ubiquitination of astrocytic Cx43 after hemin stimulation by conducting immunoprecipitation with an anti-Cx43 antibody and anti-ubiquitin antibody to clarify the process by which Cx43 is ubiquitinated. Cx43 ubiquitination was enhanced by Gap19 treatment in hemin-stimulated astrocytes (Figure 5F). These results indicate that Gap19 promotes Cx43 degradation through the ubiquitin-proteasome system in an in vitro model of ICH injury.

Gap19 increases the activity of YAP in astrocytes after ICH injury in vitro

A previous study showed that Cx43 may regulate YAP nuclear translocation in cultured astrocytes after hemoglobin stimulation[27]. Furthermore, YAP deletion has been demonstrated to lead to excessive activation of astrocytes during the development of the nervous system[28]. Additionally, prior research has demonstrated that YAP can be sequestered at the cellular junction and may regulate cell-cell interactions[19].We speculate that the pharmacological action of Gap19 in inhibiting the activation of astrocytes, which results in anti-inflammatory effects, may be associated with the interaction between astrocytic Cx43 and YAP after ICH injury.Our immunofluorescence staining results showed that YAP was mainly expressed in astrocytes but that there was almost no YAP expression in neurons and microglia (Figure 6A); this is consistent with the findings of Zhihui Huang et al[28].The activity of YAP depends on its phosphorylation state. The expression levels of YAP and phosphorylated YAP in astrocytes after hemin stimulation were detected by WB. In addition to causing Cx43 overexpression, hemin stimulation significantly increased phosphorylated YAP expression levels in astrocytes compared to those in the control group (P <0.01, Figure 6B, C), while YAP immunofluorescence showed a slight increase in YAP nuclear translocation (Figure 6 D).Intriguingly, compared to no treatment, Gap19 treatment reduced the expression of Cx43 (P<0.05), and significant decreased the level of phosphorylated YAP(P<0.05). Immunofluorescence staining showed a marked increase in YAP nuclear translocation after Gap19 treatment (Figure 6B-D). Furthermore, we evaluated the expression of YAP in the nucleus and cytoplasm. The data confirmed our hypothesis that Gap19 significantly increases nuclear YAP expression (P<0.05) and decreases cytoplasmic YAP expression (P<0.05, Figure 5E, F). These results indicate that the Cx43 mimetic peptide Gap19, which selectively blocks Cx43Hcs, may inhibit the proinflammatory function of reactive astrocytes by regulating the activity of YAP in hemin-stimulated astrocytes.

Gap19 physically regulates the association between astrocytic Cx43 and YAP in the cytoplasm after hemin stimulation

To further clarify the Cx43-YAP interaction in hemin-stimulated astrocytes, we carried overexpressed Cx43 with lentivirus to observe the subsequent changes in YAP nuclear translocation under different experimental conditions. Compared with LV-con,Lv-Cx43 effectively upregulated the expression of Cx43 and reversed the inhibition of Cx43 expression by Gap19 treatment (Figure 7A,B).Consistent with a prior study, overexpression of Cx43 significantly increased the cytoplasmic expression of YAP while decreasing nuclear YAP levels (P<0.01, Figure 7A, B).Intriguingly,after Gap19 treatment, Lv-Cx43 did not effectively inhibit YAP nuclear translocation in hemin-stimulated astrocytes (P>0.05, Figure 7A, B).These results suggest that Gap19 may intervene in the association between astrocytic Cx43 and YAP in the cytoplasm under pathological conditions. Gap19-biotin was employed in our study to pull down bound proteins with anti-biotin magnetic beads. The results confirmed that astrocytic Cx43 but not YAP interacted with Gap19(Figure 7C). To evaluate whether Gap19 disturbs the physical association between astrocytic Cx43 and YAP in the cytoplasm after hemin stimulation, a coimmunoprecipitation assay and PLA were performed.After extracting astrocytic cytoplasmic proteins,we used anti-Cx43 and anti-YAP antibodies to pull down bound proteins. Coimmunoprecipitation assays indicated that Cx43 directly bound to YAP in the astrocytic cytoplasm, but that Gap19 almost completely disrupted their interaction (Figure 7D, E). Furthermore, PLA confirmed that the interaction between Cx43 and YAP in the astrocytic cytoplasm was enhanced by hemin stimulation and Cx43 overexpression. Gap19 significantly inhibited the above association,as evidenced by the significantly decreased intensity of red fluorescence in Gap19-treated astrocytes compared to control astrocytes (Figure 7F).These results indicate that Gap19 plays a different role in disturbing the physical association between astrocytic Cx43 and YAP in the cytoplasm after hemin stimulation.

Gap19 regulates the Cx43-YAP-SOCS axis in reactive astrocytes after ICH injury.

Recent evidence has illustrated that the YAP-SOCS1/SOCS3 axis inactivates proinflammatory pathways in reactive astrocytes and regulates reactive astrogliosis under pathological conditions[28]. In this study, we detected the expression levels of SOCS1 and SOCS3 in cultured astrocytes.The results showed that the expression of SOCS1 and SOCS3 was increased in the hemin groups compared with the control group or Gap19 group (P<0.05, Figure 8A, B). However, Gap19 treatment significantly increased the expression levels of SOCS1 and SOCS3 compared with those in the hemin group (P<0.01, Figure 4A, B). Furthermore, the core markers of the TLR4-NFκB and JAK2-STAT3 pathways,which are known to be inactivated by SOCS1 and SOCS3, were measured by WB.Intriguingly,Gap19 downregulated the overexpression of TLR4,p-IKKβ and p-p65 following hemin stimulation (P<0.01, Figure 8C, D). Additionally, compared to no treatment, Gap19 downregulated the overexpression of p-JAK2 and p-STAT3 in hemin-stimulated reactive astrocytes (P<0.01, Figure 8E, F). These results suggest that Gap19 may inhibit inflammatory responses and astrocyte activation via the Cx43-YAP-SOCS1/SOCS3 axis to inhibit the TLR4-NF-κB and JAK2-STAT3 pathways in reactive astrocytes after hemin stimulation.

The YAP inhibitor VP reverses the protective effect of Gap19 after ICH injury

To further investigate whether the YAP-SOCS1/SOCS3 axis mediates the protective effects of Gap19, the widely accepted YAP inhibitor VP was employed. Previous studies have explored whether VP inhibits reactive astrogliosis in a dose-dependent manner after ICH injury. VP (5 µM/mL) was administered in vitro at the beginning of hemin stimulation. Consistent with our hypothesis, VP reversed the increase in astrocytic SOCS1/SOCS3 levels induced by Gap19 after hemin stimulation (P<0.05, Figure 9A, B). Mechanistically,the ability of Gap19 to activate the TLR4-NFκB and JAK2-STAT3 pathways was blocked by VP interference(P<0.05, Figure 9C-F). Furthermore, the transcriptional activity of inflammatory cytokines and chemokines, including IL-1β, IL-6, TNF-α and MCP-1, were significantly upregulated in the Gap19 + hemin + VP group compared with the Gap19+hemin group (Figure 9G).

In the in vivo ICH model, we treated mice with VP (0.1 mg/kg body weight, injected into the lateral ventricle once a day for 3 consecutive days. Hematoma volume and behavior were evaluated after ICH damage. Their was no brain damage or neurological deficits in the sham,Gap19 and VP groups (P>0.05, Figure 10A-F). As expected, VP treatment almost abolished the neuroprotective effect of Gap19 against ICH injury.LFB staining showed that compared with Gap19 treatment alone, inhibition of YAP signaling by VP increased the hematoma volume and reduced the blue-stained area in the mouse brain sections (P<0.05, Figure 10A, B). The neurobehavioral assessments showed that mNSSs, balance beam scores and foot faults rates were increased and that grip strength of the forelimbs was decreased in the TAT-Gap19+ICH+VP group compared with the TAT-Gap19+ICH group (Figure 10C-F). These data indicate that the anti-inflammatory and neuroprotective effects of the Cx43 mimetic peptide Gap19 after ICH injury in vitro and in vivo are mediated by YAP signaling.

Discussion

Gap junctions are specialized cell-to-cell contacts that enhance crosstalk between cells and the pericellular space[29]. In the CNS, GJCs, which are composed of two Hcs on each cell, allow the exchange of multiple substances between the cytoplasm of one cell and the cytoplasm of adjacent cells[30]. Importantly,the opening and closing of GJCs or Hcs depend on the response to stimuli such as other cellular membrane channels[31]. Connexin proteins are the necessary components of GJCs and Hcs, and Cx43 is one of the most abundant members of the connexin protein family[32]. In recent years, studies have indicated that Cx43-containing GJCs and Hcs are the main cell adhesion channels in astrocytes and maintain the homeostasis of the neural microenvironment in the CNS[10]. However, abnormal opening of Cx43Hcs on the surface of reactive astrocytes can release small molecules into the intercellular space under pathological conditions[33].These small molecules influence the steady state of the cell microenvironment, which induces inflammatory and cell death programs by regulating the crosstalk between reactive astrocytes and other cells in the CNS[34]. Definite evidence has shown that like Cx43 overexpression, abnormal Cx43Hc opening leads to further brain damage in different CNS diseases.Suppressing pathological Cx43 expression can reduce the formation of hemichannels and promote the production of survival genes[35, 36].Inhibition of Cx43Hcs with selective blockers has been shown to provide protective effects under different pathological stresses[37].Our previous research confirmed that Cx43Hc blockers significantly alleviate neurological deficits and infarct volume in a rodent

model of ischemic stroke[12, 38].To our knowledge,there have been no reports on the characteristics of Cx43Hcs after ICH injury.In our current study, sustained overexpression of Cx43 coupled with abnormal opening of Cx43Hcs was observed in a mouse model of ICH injury (Figure 1).Delayed treatment with the selective Cx43Hc blocker TAT-Gap19 for three days after ICH injury significantly blocked the excessive opening of Cx43Hcs and reduced neuronal apoptosis and white matter damage.Gap19 significantly alleviated the hematoma volume and neurological deficits after ICH injury (Figure 2).Therefore,our study is the first demonstrate that inhibiting abnormal Cx43Hc opening is a feasible strategy for treating ICH injury.

Although multiple pathological mechanisms are involved in ICH, increasing evidence has demonstrated that the inflammatory response is the main contributor to ICH progression[39]. Inflammatory mediators, including cytokines and chemokines, are produced and released by different brain cells after ICH-induced stress.These inflammatory mediators aggravate brain damage by promoting the inflammatory cascade, resulting in the further recruitment and activation of immune cells during ICH[40].Therefore,inhibiting the neuroinflammatory cascade has become an effective therapeutic strategy for ICH injury. Previous studies have shown that overexpression of Cx43 coupled with excessive Cx43Hcs opening aggravates the local inflammatory response in the CNS[41]. Inflammatory factors such as ATP,NADH and PGE2 are released into the extracellular space through Cx43Hcs, leading to the activation of intracellular inflammatory pathways[42]. However, coupled with partial Cx43 deletion, Cx43 mimetic peptides or Cx43 antisense oligodeoxynucleotides inhibit spinal cord injury by reducing proinflammatory cytokine levels[43]. Consistent with these results, we found that proinflammatory mediators, including IL-1β,IL-6,TNFα and MCP-1, were downregulated in TAT-Gap19-treated ICH mice compared to untreated mice, while anti-inflammatory cytokines, including IL-4 and IL-10, were upregulated (Figure 3). Taken together, these results suggest that ICH injury induces abnormal excessive Cx43Hc opening, which causes an increase in neuroinflammatory responses, and that this elevation is reversed by Gap19 treatment.

Astrocytes can be activated after ICH injury, and astrocyte activation is called reactive astrogliosis[44].Recently,reactive astrocytes were identified to be present in the CNS under pathological environment[45, 46]. Macroscopically,the immune response can be aggravated by reactive astrocytes following different types of CNS injury, including ICH, due to their ability to secrete chemokines and cytokines that diffuse from the injury site to the surrounding regions[47, 48].Microscopically, reactive astrocytes influence the activation of other immune cells, including microglia and macrophages, to increase the inflammatory cascade in the neural microenvironment[49].Additionally, much evidence has shown that reactive astrocytes play a vital role in crosstalk with microglia by releasing cytokines,chemokines and small molecules that influence the inflammatory response after ICH injury[50].Therefore,inhibiting the proinflammatory function of reactive astrocytes and the inflammatory cascade that results from acute astrocyte activation can alleviate inflammatory responses after ICH injury.Cx43, the most abundant gap junction protein in astrocytes, regulates astrogliosis function in the CNS[14].Cx43 overexpression coupled with excessive Cx43Hc opening contributes to astrocyte reactive migration, leading to increased neuroinflammation[51].Vignal N et al reported that astrocytic Cx43 deficiency protects against lipopolysaccharide (LPS)-induced inflammation in the CNS[52]. Kim Y's team

showed that blocking astrocytic Cx43Hcs with tonabersat can significantly inhibit local inflammation in the CNS[53].Additionally,CX43 upregulation, which activates astrocytic Hcs, has been observed under inflammatory conditions in hSOD^{G93A} mice (an ALS mouse model).Additionally,pharmacological blockade of Cx43 by Hc blockers reduces the inflammatory response and exerts protective effects in cocultured motor neurons and hSOD^{G93A} astrocytes[54].In this study, abnormal Cx43 overexpression and excessive Cx43Hc opening were mainly detected in astrocytes rather than neurons or microglia after hemin stimulation in vitro (Figures 3 and 5).In addition to reversing Cx43 overexpression and excessive Cx43Hc opening in astrocytes,Gap19 significantly decreased astrocyte activation after ICH injury in vitro and vivo, as determined by staining for GFAP, a hallmark of reactive astrogliosis (Figure 3). Furthermore, Gap19 treatment reduced proinflammatory cytokine production and release by reactive astrocytes (Figure 4). Consistent with our previous study in a mouse model of cerebral ischemic stroke, our present data demonstrated that astrocyte activation and proinflammatory effects after ICH injury were regulated by Cx43 or Cx43Hcs.However,the mechanism by which astroglial function is altered by the Cx43 mimetic peptide needs to be further evaluated.

Ubiquitination is an important pathway underlying membrane protein degradation in both physiological and pathological states[55].Conclusively,the degradation of Cx43 by the ubiquitin-proteasome system has been demonstrated to determine the fate of gap junctions[56].The proteasomal degradation of Cx43 was first explored by evaluating the effects of the proteasome inhibitor MG132, which enhances the stabilization of Cx43 at the plasma membrane[57].However,Cuervo's team showed that the macroautophagy contributes to the ubiquitination of Cx43 during serum starvation[58]. This discrepancy may have resulted from the induction of different types of posttranslational modification of Cx43 by different stimuli.In our previous study, Cx43 mimetic peptides, including Gap26 and Gap27, were shown to increase the degradation of astrocytic Cx43 through the ubiquitin-proteasome pathway in culture after oxygen-glucose deprivation[59, 60]. Intriguingly,we also showed that Gap19 has pharmacological effects in reducing the expression levels of astroglial Cx43 after cerebral ischemia injury.In this study,the transcriptional activity and expression of Cx43 in astrocytes were significantly increased in culture after hemin stimulation.However,Gap19 treatment downregulated the expression of astrocytic Cx43 but did not influence the transcriptional activity of Cx43 after hemin stimulation, revealing that Gap19 reduced the stability of Cx43. As expected, Gap19 enhanced the ubiquitination of astrocytic Cx43 after hemin stimulation.Intriguingly,the downregulation of astrocytic Cx43 by Gap19 was reversed by MG132 but not chloroquine (a lysosomal inhibitor), which suggests that the ubiquitin-proteasome pathway may contribute to the abovementioned pharmacological phenomenon. These results strongly suggest that Cx43 ubiquitination was increased by Gap19 treatment (Figure 5).However,the detailed mechanism of how Gap19 regulates the ubiquitination of astrocytic Cx43 after ICH injury still requires further study. We speculate that Gap19, as a mimetic peptide of Cx43, may influence the sites of astrocytic Cx43 posttranslational modification under pathologic conditions.

The proinflammatory mechanisms of astrocytic Cx43 in CNS diseases are still unclear. However, increasing evidence has demonstrated that blockers of Cx43Hcs can regulate many intracellular

signaling pathways.Yin et al showed that carbenoxolone and Gap26, blockers of Cx43Hcs, significantly inhibit neuroinflammation in an astrocytic ischemia model by regulating PKC,PKB and Src signaling in both the membrane and cytoplasm[24].Li et al found that the Cx43 mimetic peptides Gap26 and Gap27 promote cytoplasmic degradation of astroglial Cx43 via the PI3K/Akt pathway in neonatal rats after ischemic brain injury[38]. Our previous study also found that Gap19 exerts its anti-inflammatory effects by inhibiting the activation of the JAK2/STAT3 and TLR4 signaling pathways in astrocytes after cerebral ischemic stroke[11, 12]. Consistent with these results, we believe that modulating intracellular signaling pathways may change the function of astrocytic Cx43 on the cellular plasma membrane.

The Hippo signaling pathway plays a key role in tissue homeostasis, tissue regeneration and organ size regulation. Early studies showed that abnormal Hippo signaling contributes to the development of tumors[61].Recently, mounting evidence has shown the important role of Hippo/YAP signaling in CNS homeostasis. Dysfunction of Hippo/YAP signaling contributes to negative proapoptotic and proinflammatory effects in CNS diseases[16]. During cerebral ischemic injury,YAP deletion aggravates BBB and astrocyte damage.MST1,another important regulator of YAP in the Hippo pathways, is overactivated in a model of ICH, and knocking down MST1 mitigates inflammatory reactions and neuronal cell death[62]. Recently, the functions of YAP signaling in astrocytes were evaluated. Abnormal reactive astrogliosis and microglial activation are observed in YAP knockout mice during cerebral development.Hence,astroglial YAP deletion leads to excessive activation of inflammatory pathways, which seems to aggravate dysfunction of astrocytes and the proinflammatory effects of reactive astrogliosis[28, 63].Interestingly,YAP has been shown to play an important role in regulating cellular junctions. Inhibition of its transcriptional activity at the plasma membrane can disrupt cellular contacts[64].Yang et al found that astrocytic Cx43 reduces the nuclear translocation of YAP in a hemoglobin mouse model[27]. These studies suggest that the proinflammatory functions of astroglial Cx43 and Cx43Hcs may be associated with YAP signaling in ICH injury. To verify the above hypothesis, we designed various experiments. The results first showed that even after ICH,YAP expression was more abundant in astrocytes than in neurons and microglia. Cx43overexpression was accompanied by an increased level of phosphorylated YAP in cultured reactive astrocytes after hemin stimulation. In contrast, Gap19 decreased astroglial Cx43 levels, the level of phosphorylated YAP was decreased, and YAP nuclear translocation was significantly increased (Figure 6).We speculated that the protective effects of Gap19 may be mainly associated with its ability to regulate the degradation of cytoplasmic Cx43, which triggers YAP nuclear translocation in cultured astrocytes after hemin stimulation.However, surprisingly, Cx43 overexpression did not reverse YAP nuclear translocation after Gap19 treatment.In the follow-up experiments, coimmunoprecipitation and PLA revealed that Gap19 interrupts the physical association between Cx43 and YAP in the astrocytic cytoplasm. To our knowledge, this is the first investigation to explore the interaction between Cx43 and YAP following Gap19 treatment (Figure 7).These data indicate that the functional changes in astrocytic Cx43 and Cx43Hcs may be associated with the Cx43-YAP interaction, which contributes to astrocyte activation and regulates the inflammatory response after ICH injury.

Recent evidence has shown that the transcriptional activity of SOCS family members, including SOCS1 and SOCS3, in astrocytes is regulated by YAP signaling[28].Multiple studies have confirmed that SOCS1 and SOCS3 overexpression inhibits the inflammatory TLR4-NFκB and JAK-STAT pathways in CNS diseases[65]. In this study, following hemin stimulation, the expression of SOCS1 and SOCS3 in astrocytes was decreased, while the inflammatory the TLR4-NFκB and JAK2-STAT3 pathways were activated.Gap19 reversed the downregulation of the two proteins in hemin-stimulated astrocytes. The inflammatory TLR4-NFκB and JAK2-STAT3 pathways were also inhibited by Gap19 treatment (Figure 8). Finally,VP, a nuclear YAP activity inhibitor,was applied in our study.VP not only reversed the anti-inflammatory effect in vitro but also almost completely blocked the protective effects of Gap19 in vivo after ICH injury (Figures 9 and 10). Therefore,our results reveal that the protective effects of Gap19 in blocking Cx43Hcs may be associated with functional changes in the Cx43-YAP-SOCS axis in reactive astrocytes after ICH injury.

Conclusion

In summary, our findings are the first to demonstrate that abnormal Cx43 overexpression and excessive Cx43Hc opening aggravates brain tissue damage and neurological deficits after ICH injury. The Cx43 mimetic peptide Gap19 has neuroprotective effects in an ICH animal model. Gap19 suppresses abnormal astroglial Cx43 expression and Cx43Hc opening, which inhibits astrocyte activation and the inflammatory response via YAP signaling after ICH injury. This study provides new insight into potential treatment strategies for ICH injury involving astroglial Cx43 and Cx43Hcs.

Abbreviations

CNS：central nervous system;Cx43:Connexin43 ;Cx43Hcs:Cx43 hemichannels; Co-IP:Co-immunoprecipitation;EtBr:Ethidium bromide ;FFT：Foot fault test;FJC:Fluoro-Jade C;GJCs:gap junction channels ;ICH:intracerebral hemorrhage;LFB:Luxol fast blue;mNSS:modified neurological severity score ;PLA：proximity ligation assay ;VP:verteporfin .

Declarations

Declaration of interest

No potential conflict of interest was reported by the authors.

Acknowledgment

Funding

Availability of data and materials:

All data generated or analyzed during this study are included in this published article and its supplementary information files.

Author Contributions

Conceived and designed the experiments: XY, WKY, HLY. Performed the experiments: HLY, WL, XC, JC, PYL, LLS. Analyzed the data: WL, HLY. Contributed reagents/materials/analysis tools: XC, YX. Contributed to the writing of the manuscript: HLY, WL, XC.

Ethics approval and consent to participate

All the experiments involving animals were approved by the Institutional Animal Care and Use Committee of Nanjing University. This study was approved by the ethics committee at Nanjing Drum Tower Hospital, Nanjing University Medical School.

Consent for publication

Not applicable.

Competing interests

The authors declare that they have no competing interests.

References

1. Al-Shahi Salman R, Frantzias J, Lee RJ, Lyden PD, Battey TWK, Ayres AM, Goldstein JN, Mayer SA, Steiner T, Wang X, et al: **Absolute risk and predictors of the growth of acute spontaneous intracerebral haemorrhage: a systematic review and meta-analysis of individual patient data.** *Lancet Neurol* 2018, **17:**885-894.
2. Cao S, Zheng M, Hua Y, Chen G, Keep RF, Xi G: **Hematoma Changes During Clot Resolution After Experimental Intracerebral Hemorrhage.** *Stroke* 2016, **47:**1626-1631.
3. Graeber MB, Li W, Rodriguez ML: **Role of microglia in CNS inflammation.** *FEBS Lett* 2011, **585:**3798-3805.

4. Wu X, Fu S, Liu Y, Luo H, Li F, Wang Y, Gao M, Cheng Y, Xie Z: **NDP-MSH binding melanocortin-1 receptor ameliorates neuroinflammation and BBB disruption through CREB/Nr4a1/NF-kappaB pathway after intracerebral hemorrhage in mice.** *J Neuroinflammation* 2019, **16**:192.

5. Giaume C, Leybaert L, Naus CC, Saez JC: **Connexin and pannexin hemichannels in brain glial cells: properties, pharmacology, and roles.** *Front Pharmacol* 2013, **4**:88.

6. Ye ZC, Wyeth MS, Baltan-Tekkok S, Ransom BR: **Functional hemichannels in astrocytes: a novel mechanism of glutamate release.** *J Neurosci* 2003, **23**:3588-3596.

7. Stout CE, Costantin JL, Naus CC, Charles AC: **Intercellular calcium signaling in astrocytes via ATP release through connexin hemichannels.** *J Biol Chem* 2002, **277**:10482-10488.

8. Jaraiz-Rodriguez M, Talaveron R, Garcia-Vicente L, Pelaz SG, Dominguez-Prieto M, Alvarez-Vazquez A, Flores-Hernandez R, Sin WC, Bechberger J, Medina JM, et al: **Connexin43 peptide, TAT-Cx43266-283, selectively targets glioma cells, impairs malignant growth, and enhances survival in mouse models in vivo.** *Neuro Oncol* 2020, **22**:493-504.

9. Danesh-Meyer HV, Zhang J, Acosta ML, Rupenthal ID, Green CR: **Connexin43 in retinal injury and disease.** *Prog Retin Eye Res* 2016, **51**:41-68.

10. Retamal MA, Froger N, Palacios-Prado N, Ezan P, Saez PJ, Saez JC, Giaume C: **Cx43 hemichannels and gap junction channels in astrocytes are regulated oppositely by proinflammatory cytokines released from activated microglia.** *J Neurosci* 2007, **27**:13781-13792.

11. Chen Y, Wang L, Zhang L, Chen B, Yang L, Li X, Li Y, Yu H: **Inhibition of Connexin 43 Hemichannels Alleviates Cerebral Ischemia/Reperfusion Injury via the TLR4 Signaling Pathway.** *Front Cell Neurosci* 2018, **12**:372.

12. Chen B, Yang L, Chen J, Chen Y, Zhang L, Wang L, Li X, Li Y, Yu H: **Inhibition of Connexin43 hemichannels with Gap19 protects cerebral ischemia/reperfusion injury via the JAK2/STAT3 pathway in mice.** *Brain Res Bull* 2019, **146**:124-135.

13. Hawat G, Helie P, Baroudi G: **Single intravenous low-dose injections of connexin 43 mimetic peptides protect ischemic heart in vivo against myocardial infarction.** *J Mol Cell Cardiol* 2012, **53**:559-566.

14. Abudara V, Bechberger J, Freitas-Andrade M, De Bock M, Wang N, Bultynck G, Naus CC, Leybaert L, Giaume C: **The connexin43 mimetic peptide Gap19 inhibits hemichannels without altering gap junctional communication in astrocytes.** *Front Cell Neurosci* 2014, **8**:306.

15. Yu FX, Zhao B, Panupinthu N, Jewell JL, Lian I, Wang LH, Zhao J, Yuan H, Tumaneng K, Li H, et al: **Regulation of the Hippo-YAP pathway by G-protein-coupled receptor signaling.** *Cell* 2012, **150**:780-791.

16. Cheng J, Wang S, Dong Y, Yuan Z: **The Role and Regulatory Mechanism of Hippo Signaling Components in the Neuronal System.** *Front Immunol* 2020, **11**:281.

17. Taha Z, Janse van Rensburg HJ, Yang X: **The Hippo Pathway: Immunity and Cancer.** *Cancers (Basel)* 2018, **10**.

18. Sharma P, Hu-Lieskovan S, Wargo JA, Ribas A: **Primary, Adaptive, and Acquired Resistance to Cancer Immunotherapy.** *Cell* 2017, **168**:707-723.

19. Cox CM, Mandell EK, Stewart L, Lu R, Johnson DL, McCarter SD, Tavares A, Runyan R, Ghosh S, Wilson JM: **Endosomal regulation of contact inhibition through the AMOT:YAP pathway.** *Mol Biol Cell* 2015, **26:**2673-2684.

20. Freitas-Andrade M, Wang N, Bechberger JF, De Bock M, Lampe PD, Leybaert L, Naus CC: **Targeting MAPK phosphorylation of Connexin43 provides neuroprotection in stroke.** *J Exp Med* 2019, **216:**916-935.

21. Maatouk L, Yi C, Carrillo-de Sauvage MA, Compagnion AC, Hunot S, Ezan P, Hirsch EC, Koulakoff A, Pfrieger FW, Tronche F, et al: **Glucocorticoid receptor in astrocytes regulates midbrain dopamine neurodegeneration through connexin hemichannel activity.** *Cell Death Differ* 2019, **26:**580-596.

22. Matsushita H, Hijioka M, Ishibashi H, Anan J, Kurauchi Y, Hisatsune A, Seki T, Shudo K, Katsuki H: **Suppression of CXCL2 upregulation underlies the therapeutic effect of the retinoid Am80 on intracerebral hemorrhage in mice.** *J Neurosci Res* 2014, **92:**1024-1034.

23. Gao L, Lu Q, Huang LJ, Ruan LH, Yang JJ, Huang WL, ZhuGe WS, Zhang YL, Fu B, Jin KL, ZhuGe QC: **Transplanted neural stem cells modulate regulatory T, gammadelta T cells and corresponding cytokines after intracerebral hemorrhage in rats.** *Int J Mol Sci* 2014, **15:**4431-4441.

24. Yin X, Feng L, Ma D, Yin P, Wang X, Hou S, Hao Y, Zhang J, Xin M, Feng J: **Roles of astrocytic connexin-43, hemichannels, and gap junctions in oxygen-glucose deprivation/reperfusion injury induced neuroinflammation and the possible regulatory mechanisms of salvianolic acid B and carbenoxolone.** *J Neuroinflammation* 2018, **15:**97.

25. Quintana FJ: **Astrocytes to the rescue! Glia limitans astrocytic endfeet control CNS inflammation.** *J Clin Invest* 2017, **127:**2897-2899.

26. Zhang FF, Morioka N, Kitamura T, Hisaoka-Nakashima K, Nakata Y: **Proinflammatory cytokines downregulate connexin 43-gap junctions via the ubiquitin-proteasome system in rat spinal astrocytes.** *Biochem Biophys Res Commun* 2015, **464:**1202-1208.

27. Yang Y, Ren J, Sun Y, Xue Y, Zhang Z, Gong A, Wang B, Zhong Z, Cui Z, Xi Z, et al: **A connexin43/YAP axis regulates astroglial-mesenchymal transition in hemoglobin induced astrocyte activation.** *Cell Death Differ* 2018, **25:**1870-1884.

28. Huang Z, Wang Y, Hu G, Zhou J, Mei L, Xiong WC: **YAP Is a Critical Inducer of SOCS3, Preventing Reactive Astrogliosis.** *Cereb Cortex* 2016, **26:**2299-2310.

29. Charles AC, Naus CC, Zhu D, Kidder GM, Dirksen ER, Sanderson MJ: **Intercellular calcium signaling via gap junctions in glioma cells.** *J Cell Biol* 1992, **118:**195-201.

30. Willecke K, Eiberger J, Degen J, Eckardt D, Romualdi A, Guldenagel M, Deutsch U, Sohl G: **Structural and functional diversity of connexin genes in the mouse and human genome.** *Biol Chem* 2002, **383:**725-737.

31. Jiang JX, Cherian PP: **Hemichannels formed by connexin 43 play an important role in the release of prostaglandin E(2) by osteocytes in response to mechanical strain.** *Cell Commun Adhes* 2003, **10:**259-264.

32. Wang J, Yang ZY, Guo YF, Kuang JY, Bian XW, Yu SC: **Targeting different domains of gap junction protein to control malignant glioma.** *Neuro Oncol* 2018, **20:**885-896.

33. Vicario N, Zappala A, Calabrese G, Gulino R, Parenti C, Gulisano M, Parenti R: **Connexins in the Central Nervous System: Physiological Traits and Neuroprotective Targets.** *Front Physiol* 2017, **8:**1060.

34. Liu X, Gangoso E, Yi C, Jeanson T, Kandelman S, Mantz J, Giaume C: **General anesthetics have differential inhibitory effects on gap junction channels and hemichannels in astrocytes and neurons.** *Glia* 2016, **64:**524-536.

35. Orellana JA, Hernandez DE, Ezan P, Velarde V, Bennett MV, Giaume C, Saez JC: **Hypoxia in high glucose followed by reoxygenation in normal glucose reduces the viability of cortical astrocytes through increased permeability of connexin 43 hemichannels.** *Glia* 2010, **58:**329-343.

36. Gajardo-Gomez R, Labra VC, Maturana CJ, Shoji KF, Santibanez CA, Saez JC, Giaume C, Orellana JA: **Cannabinoids prevent the amyloid beta-induced activation of astroglial hemichannels: A neuroprotective mechanism.** *Glia* 2017, **65:**122-137.

37. Manjarrez-Marmolejo J, Franco-Perez J: **Gap Junction Blockers: An Overview of their Effects on Induced Seizures in Animal Models.** *Curr Neuropharmacol* 2016, **14:**759-771.

38. Li X, Zhao H, Tan X, Kostrzewa RM, Du G, Chen Y, Zhu J, Miao Z, Yu H, Kong J, Xu X: **Inhibition of connexin43 improves functional recovery after ischemic brain injury in neonatal rats.** *Glia* 2015, **63:**1553-1567.

39. Zhou Y, Wang Y, Wang J, Anne Stetler R, Yang QW: **Inflammation in intracerebral hemorrhage: from mechanisms to clinical translation.** *Prog Neurobiol* 2014, **115:**25-44.

40. Xi G, Keep RF, Hoff JT: **Mechanisms of brain injury after intracerebral haemorrhage.** *Lancet Neurol* 2006, **5:**53-63.

41. Boulay AC, Cisternino S, Cohen-Salmon M: **Immunoregulation at the gliovascular unit in the healthy brain: A focus on Connexin 43.** *Brain Behav Immun* 2016, **56:**1-9.

42. Locovei S, Scemes E, Qiu F, Spray DC, Dahl G: **Pannexin1 is part of the pore forming unit of the P2X(7) receptor death complex.** *FEBS Lett* 2007, **581:**483-488.

43. O'Carroll SJ, Gorrie CA, Velamoor S, Green CR, Nicholson LF: **Connexin43 mimetic peptide is neuroprotective and improves function following spinal cord injury.** *Neurosci Res* 2013, **75:**256-267.

44. Eroglu C, Barres BA: **Regulation of synaptic connectivity by glia.** *Nature* 2010, **468:**223-231.

45. Xie L, Yang SH: **Interaction of astrocytes and T cells in physiological and pathological conditions.** *Brain Res* 2015, **1623:**63-73.

46. Mantovani A, Sica A, Sozzani S, Allavena P, Vecchi A, Locati M: **The chemokine system in diverse forms of macrophage activation and polarization.** *Trends Immunol* 2004, **25:**677-686.

47. Mayo L, Cunha AP, Madi A, Beynon V, Yang Z, Alvarez JI, Prat A, Sobel RA, Kobzik L, Lassmann H, et al: **IL-10-dependent Tr1 cells attenuate astrocyte activation and ameliorate chronic central nervous system inflammation.** *Brain* 2016, **139:**1939-1957.

48. Leng L, Zhuang K, Liu Z, Huang C, Gao Y, Chen G, Lin H, Hu Y, Wu D, Shi M, et al: **Menin Deficiency Leads to Depressive-like Behaviors in Mice by Modulating Astrocyte-Mediated Neuroinflammation.** *Neuron* 2018, **100:**551-563 e557.

49. Mott RT, Ait-Ghezala G, Town T, Mori T, Vendrame M, Zeng J, Ehrhart J, Mullan M, Tan J: **Neuronal expression of CD22: novel mechanism for inhibiting microglial proinflammatory cytokine production.** *Glia* 2004, **46:**369-379.

50. Lan X, Han X, Li Q, Yang QW, Wang J: **Modulators of microglial activation and polarization after intracerebral haemorrhage.** *Nat Rev Neurol* 2017, **13:**420-433.

51. Hara M, Kobayakawa K, Ohkawa Y, Kumamaru H, Yokota K, Saito T, Kijima K, Yoshizaki S, Harimaya K, Nakashima Y, Okada S: **Interaction of reactive astrocytes with type I collagen induces astrocytic scar formation through the integrin-N-cadherin pathway after spinal cord injury.** *Nat Med* 2017, **23:**818-828.

52. Vignal N, Boulay AC, San C, Cohen-Salmon M, Rizzo-Padoin N, Sarda-Mantel L, Decleves X, Cisternino S, Hosten B: **Astroglial Connexin 43 Deficiency Protects against LPS-Induced Neuroinflammation: A TSPO Brain microPET Study with [(18)F]FEPPA.** *Cells* 2020, **9**.

53. Kim Y, Griffin JM, Nor MNM, Zhang J, Freestone PS, Danesh-Meyer HV, Rupenthal ID, Acosta M, Nicholson LFB, O'Carroll SJ, Green CR: **Tonabersat Prevents Inflammatory Damage in the Central Nervous System by Blocking Connexin43 Hemichannels.** *Neurotherapeutics* 2017, **14:**1148-1165.

54. Almad AA, Doreswamy A, Gross SK, Richard JP, Huo Y, Haughey N, Maragakis NJ: **Connexin 43 in astrocytes contributes to motor neuron toxicity in amyotrophic lateral sclerosis.** *Glia* 2016, **64:**1154-1169.

55. Pickart CM, Eddins MJ: **Ubiquitin: structures, functions, mechanisms.** *Biochim Biophys Acta* 2004, **1695:**55-72.

56. Ribeiro-Rodrigues TM, Catarino S, Pinho MJ, Pereira P, Girao H: **Connexin 43 ubiquitination determines the fate of gap junctions: restrict to survive.** *Biochem Soc Trans* 2015, **43:**471-475.

57. Saez JC, Berthoud VM, Branes MC, Martinez AD, Beyer EC: **Plasma membrane channels formed by connexins: their regulation and functions.** *Physiol Rev* 2003, **83:**1359-1400.

58. Bejarano E, Girao H, Yuste A, Patel B, Marques C, Spray DC, Pereira P, Cuervo AM: **Autophagy modulates dynamics of connexins at the plasma membrane in a ubiquitin-dependent manner.** *Mol Biol Cell* 2012, **23:**2156-2169.

59. Leithe E, Rivedal E: **Ubiquitination and down-regulation of gap junction protein connexin-43 in response to 12-O-tetradecanoylphorbol 13-acetate treatment.** *J Biol Chem* 2004, **279:**50089-50096.

60. Dunn CA, Su V, Lau AF, Lampe PD: **Activation of Akt, not connexin 43 protein ubiquitination, regulates gap junction stability.** *J Biol Chem* 2012, **287:**2600-2607.

61. Chang L, Azzolin L, Di Biagio D, Zanconato F, Battilana G, Lucon Xiccato R, Aragona M, Giulitti S, Panciera T, Gandin A, et al: **The SWI/SNF complex is a mechanoregulated inhibitor of YAP and TAZ.** *Nature* 2018, **563:**265-269.

62. Zhang P, Wang T, Zhang D, Zhang Z, Yuan S, Zhang J, Cao J, Li H, Li X, Shen H, Chen G: **Exploration of MST1-Mediated Secondary Brain Injury Induced by Intracerebral Hemorrhage in Rats via Hippo Signaling Pathway.** *Transl Stroke Res* 2019, **10:**729-743.

63. He Q, Gao Y, Wang T, Zhou L, Zhou W, Yuan Z: **Deficiency of Yes-Associated Protein Induces Cataract in Mice.** *Aging Dis* 2019, **10:**293-306.

64. Zhao B, Wei X, Li W, Udan RS, Yang Q, Kim J, Xie J, Ikenoue T, Yu J, Li L, et al: **Inactivation of YAP oncoprotein by the Hippo pathway is involved in cell contact inhibition and tissue growth control.** *Genes Dev* 2007, **21:**2747-2761.

65. Cianciulli A, Calvello R, Porro C, Trotta T, Panaro MA: **Understanding the role of SOCS signaling in neurodegenerative diseases: Current and emerging concepts.** *Cytokine Growth Factor Rev* 2017, **37:**67-79.

Figures
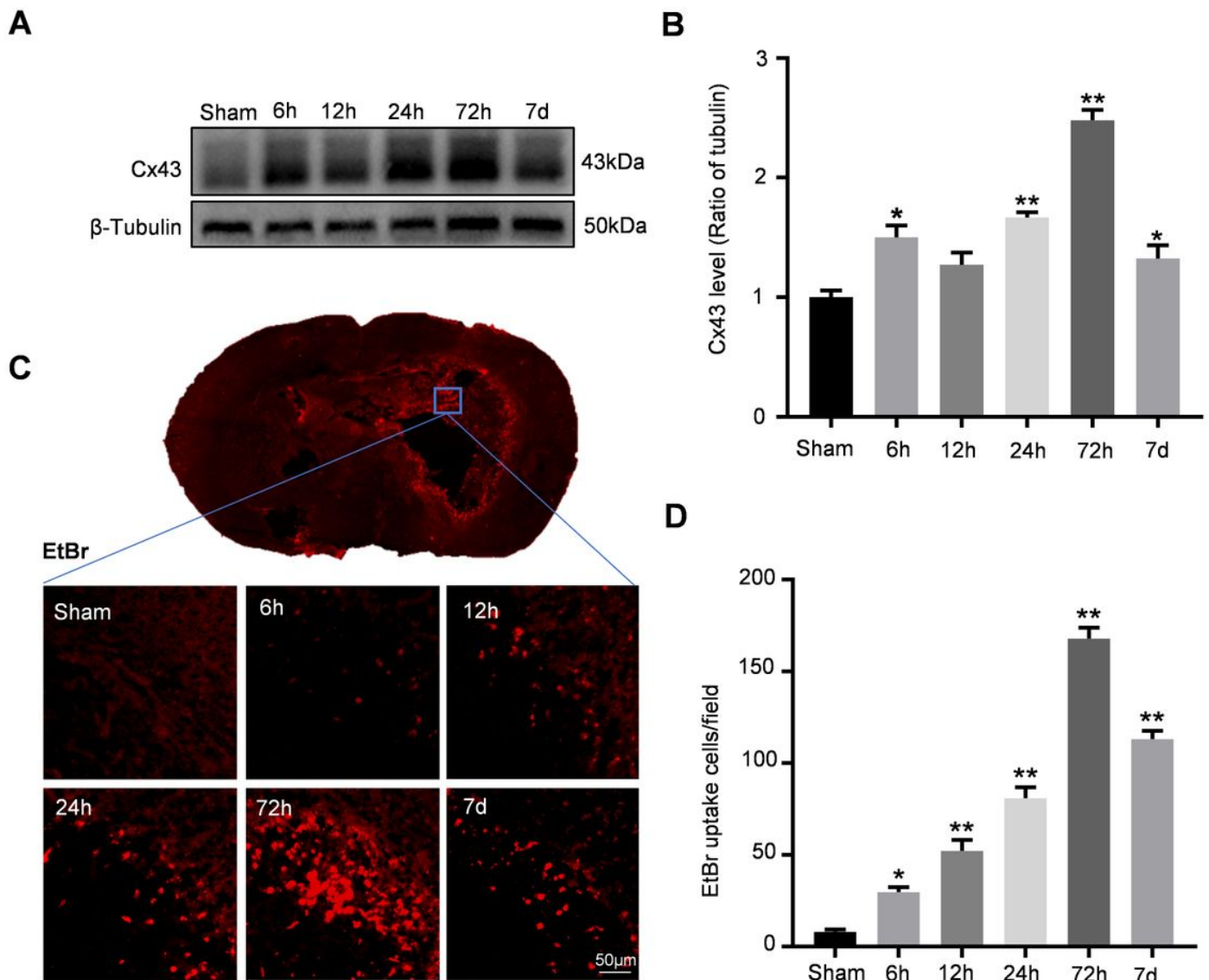
Figure 1

Expression of Cx43 at different time points and abnormal opening of Cx43Hcs after ICH injury .(A) WB analysis of the expression levels of Cx43 and β-tubulin in normal brain tissue and in brain tissue surrounding cerebral hemorrhage 6 h, 12 h, 24 h, 72 h and 7 d after ICH. (B) Quantitative analysis showing the ratio of Cx43 to β-tubulin. (C) EtBr staining was used to evaluate the opening of the Hcs and to select peripheral brain tissues, as shown in the figure. (D) EtBr staining showed that Hc opening gradually increased after ICH injury, reached a peak on 72 h (excessive Cx43Hc opening), and then gradually decreased on 7 d. The bars represent the SEM of the data from 3 brain samples per group. *, $P<0.05$, ** $P<0.01$ compared to the sham group.
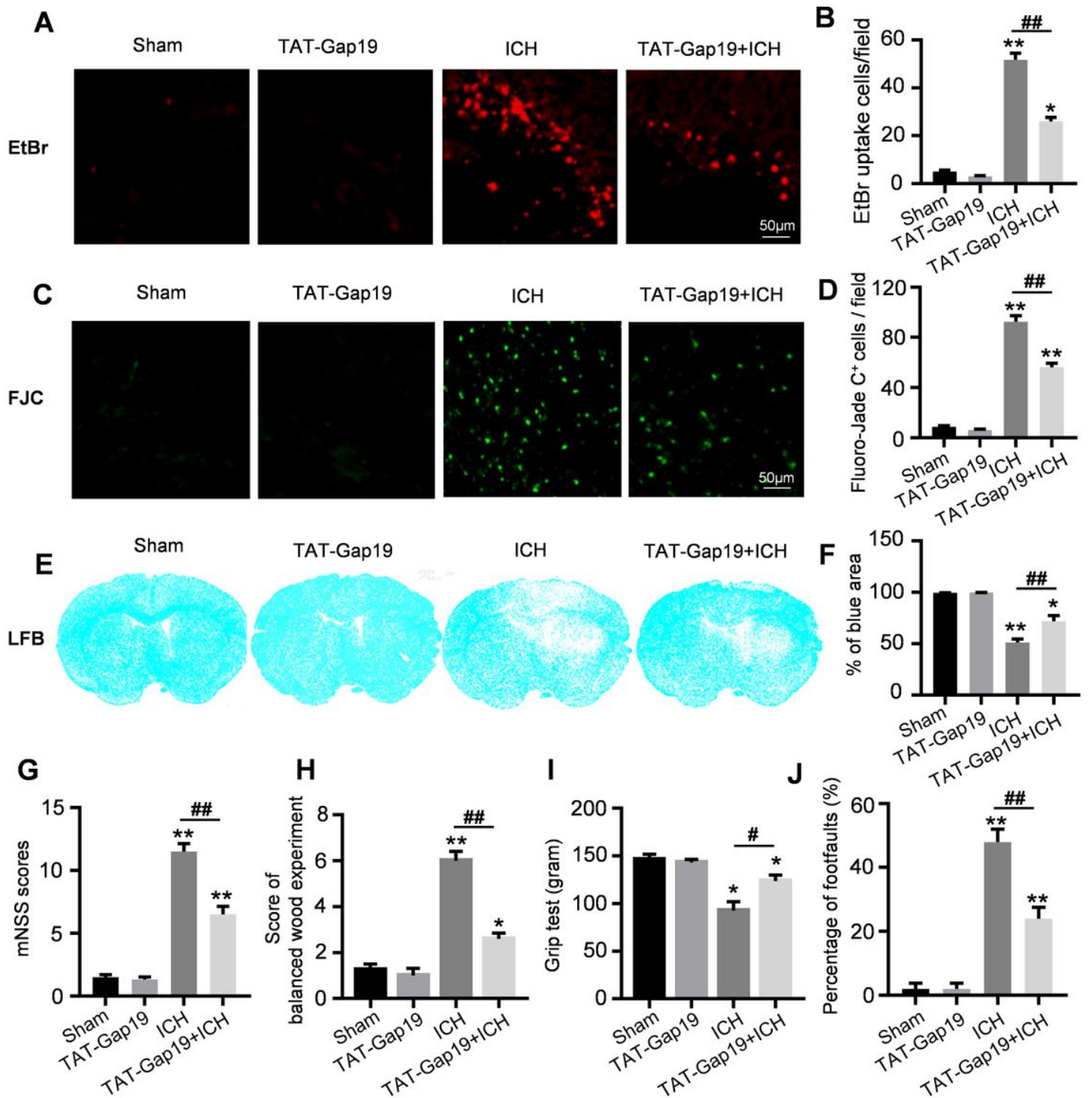
Figure 2

Gap19 blocks Cx43Hc opening and provides neuroprotection after ICH injury. (A, B) EtBr staining evaluation showed that TAT-Gap19 treatment after ICH reduced Hc opening. (C, D) The TAT-Gap19 ICH group exhibited significantly fewer apoptotic neurons than the ICH group. (E, F) TAT-Gap19 treatment reduced hematoma volumes after ICH and increased the surviving blue-stained area. (G) TAT-Gap19 treatment significantly reduced post-ICH neurological dysfunction in mice, as assessed by mNSSs. (H) The balance beam test showed that after TAT-Gap19 treatment following ICH, the balance beam score,

which reflected nerve function was significantly reduced compared with that in the ICH group. (I) In the forelimb strength test, the grip strength of the ICH group was significantly lower than that of the TAT-Gap19 + ICH group. (J) In the foot fault test, the foot fault rate of the TAT-Gap19+ICH group mice was significantly lower than that of the ICH group. The bars represent the SEM of the data from 3-6 brain tissue samples per group. *, P<0.05, ** P<0.01 compared to the sham group. #, P<0.05, ##, P<0.01 compared with the ICH group.
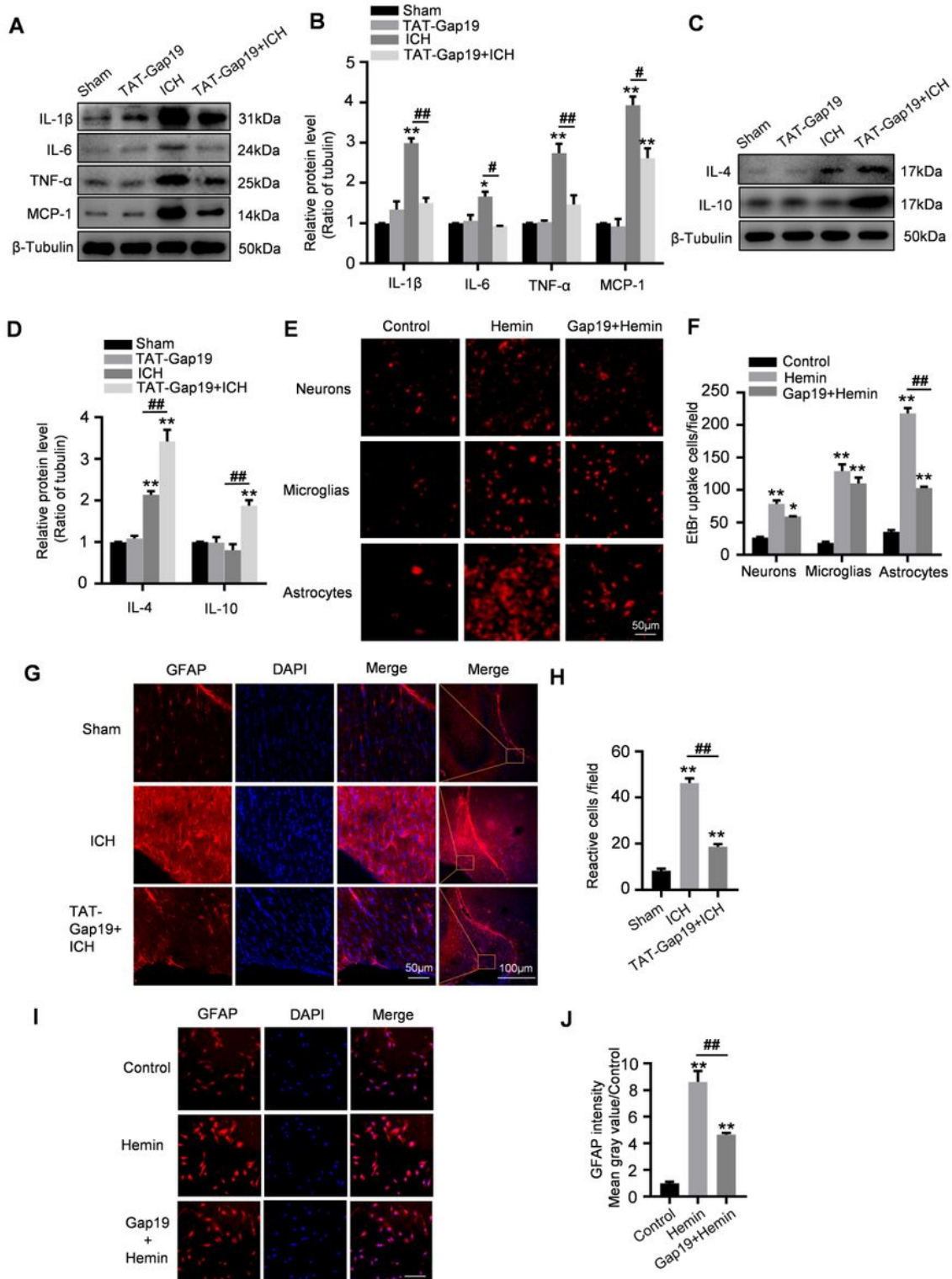
Figure 3

Gap19 reduces the expression of proinflammatory cytokines and the activation of astrocytes after ICH injury.(A, B) WB analysis showed the expression levels of TNF-a, IL-1β, IL-6, MCP1, and β-tubulin as the loading control. (C, D) The expression levels of IL-4, IL-10. β-Tubulin was used as a loading control. (E, F) The EtBr uptake assay was used to evaluate that activity of Hcs on astrocytes, microglia, and neurons after hemin stimulation.Gap19 inhibits the hemin-induced excessive opening of Hcs on astrocytes. (G, H) Immunofluorescence for GFAP was used to evaluate astrocyte activation. TAT-Gap19 treatment significantly reduced the number of GFAP-positive cells in the area surrounding the cerebral hemorrhage. (I, J) In vitro, Gap19 treatment reduced the GFAP fluorescence intensity in astrocytes after hemin stimulation. The bars in the A-D, G, and H represent the SEM of the data from 3 cerebral hemorrhage tissue samples per group. *, P<0.05, ** P<0.01 compared to the sham group. #, P<0.05, ##, P<0.01 compared with the ICH group. The bars in E, F, I, J in the ICH group represent the SEM of data from 3 samples per group. *, P<0.05, ** P<0.01 compared to the control group. #, P<0.05, ##, P<0.01 compared with the hemin group.
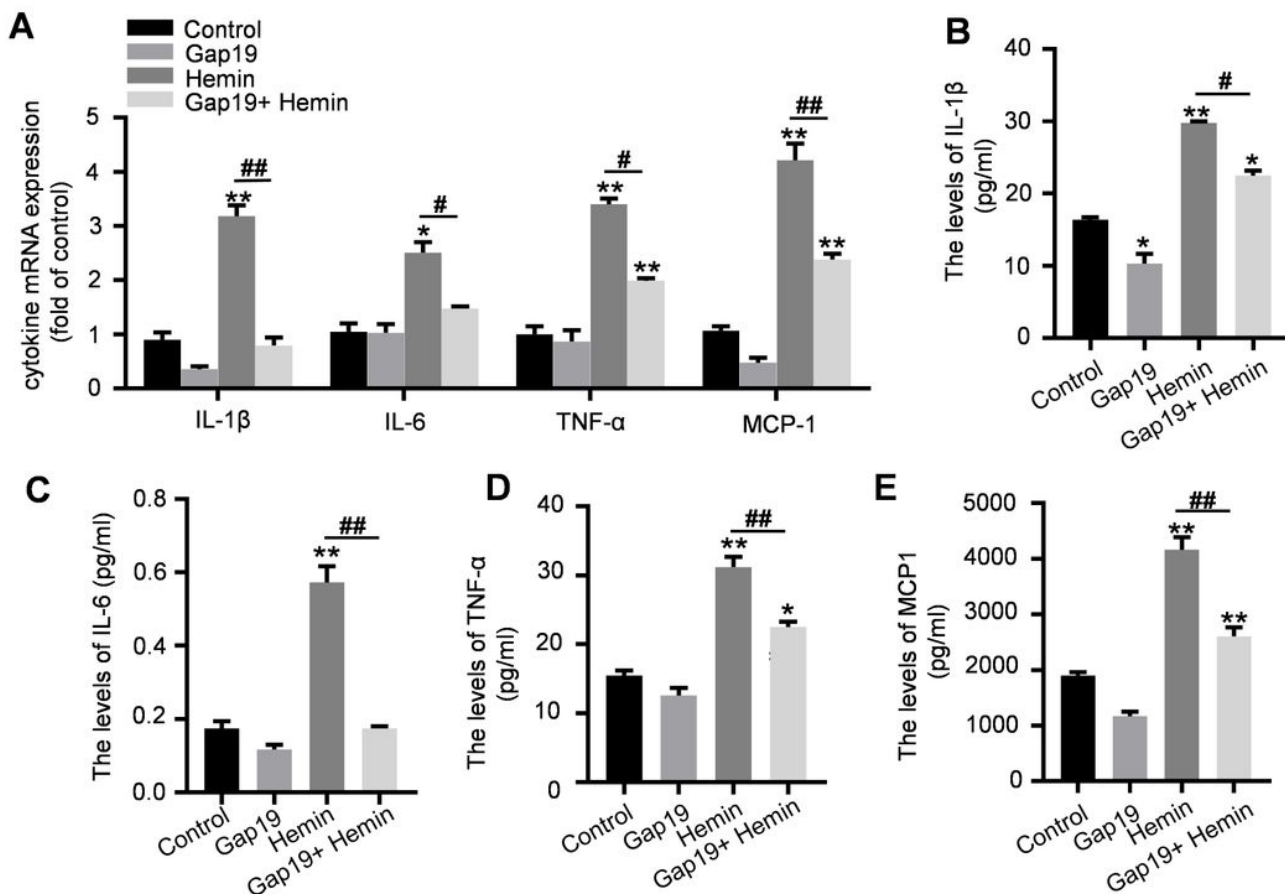
Figure 4

Gap19 reduces the production and release of proinflammatory cytokines by astrocytes after ICH injury. (A) qRT-PCR analysis of the transcriptional activities of IL-1β, IL-6, TNF-α and MCP-1 in astrocytes .(B-E) ELISA was used to detect the release of IL-1β, IL-6, TNF-α and MCP1 from astrocytes to the supernatant

following different treatments. The bars represent the SEM of data from 3 samples per group. *, P<0.05, ** P<0.01 compared to the control group. #, P<0.05, ##, P<0.01 compared with the hemin group.
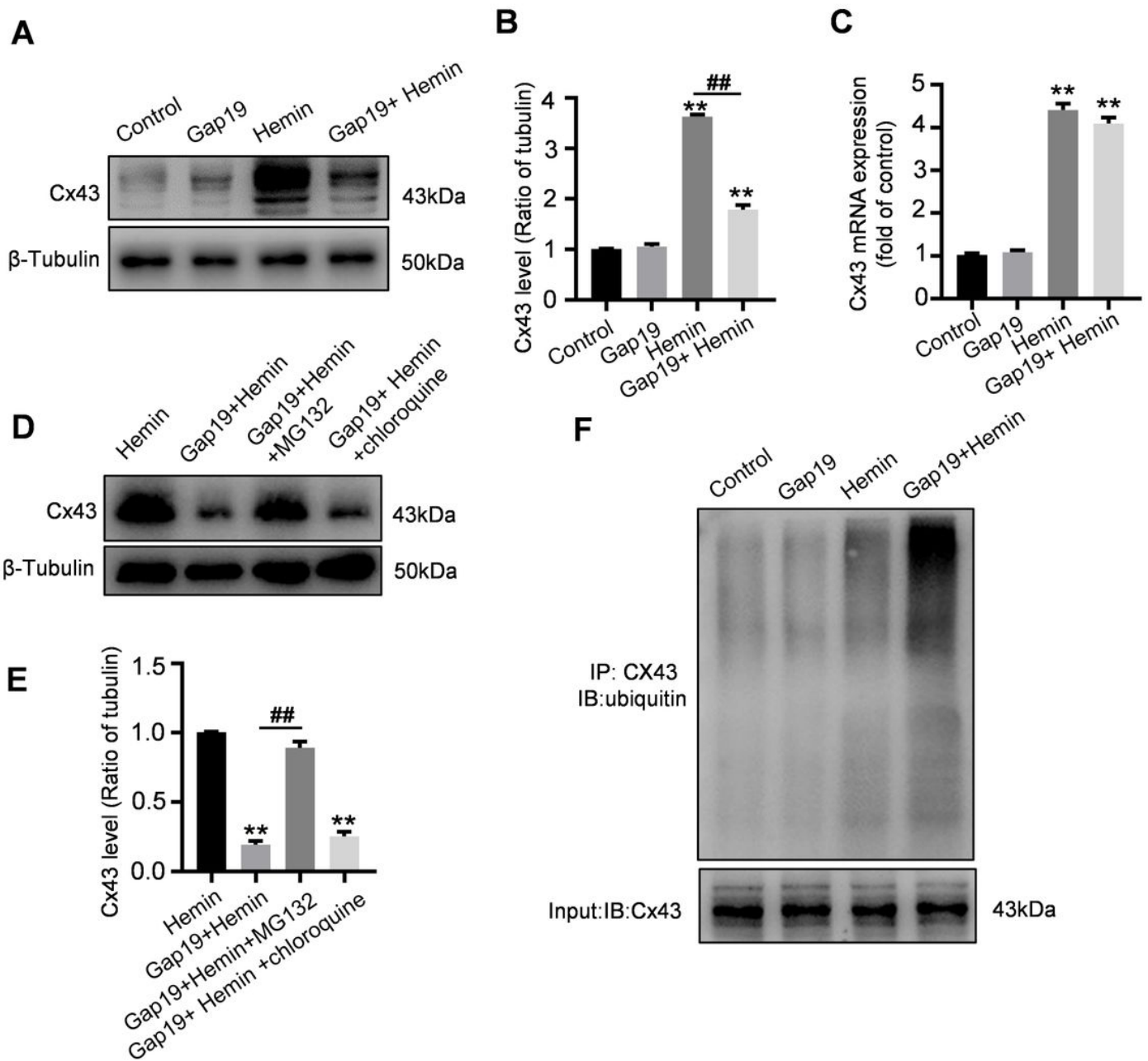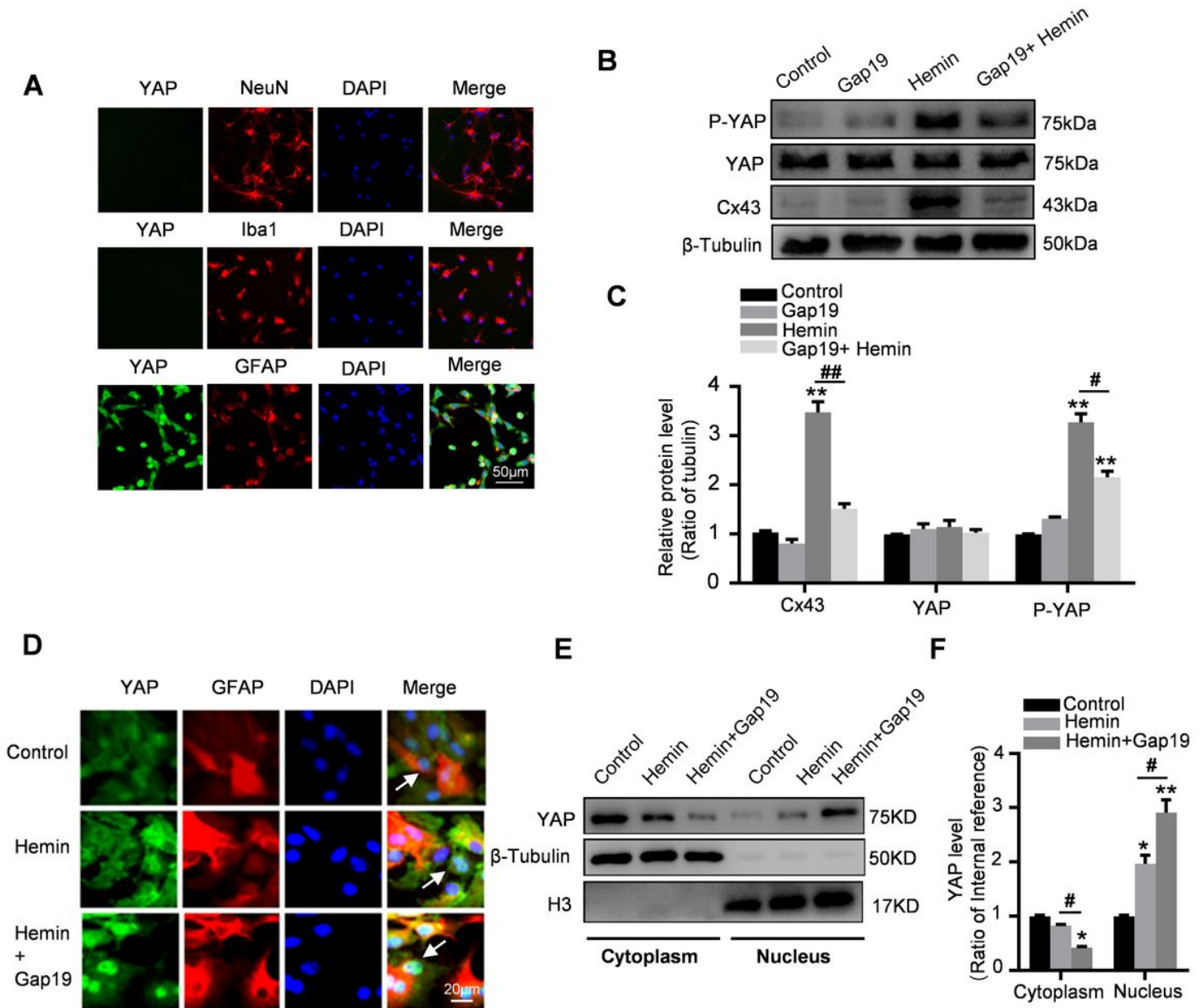

Figure 5

Gap19 promotes the degradation of astrocytic Cx43 through the ubiquitin-proteasome pathway after hemin stimulation.(A, B) WB analysis showed that Gap19 treatment reduced theCx43 levels induced by hemin stimulation. (C) RT-PCR analysis showed that after hemin stimulation, Gap19 treatment had no effect on hemin stimulation-induced Cx43 transcriptional activity. (D, E) Treating cultured astrocytes with MG132 and chloroquine for 12 h. WB analysis showed that MG132 increased the expression of Cx43 after Gap19 treatment(P<0.05), but there was no significant different of Cx43 level between chloroquine-treated group and Gap19 + hemin group. (F) Coimmunoprecipitation with an anti-Cx43 antibody was

used to analysis the ubiquitination of Cx43 in astrocytes after hemin stimulation. This figure shows that Gap19 treatment increased the level of Cx43 ubiquitination in astrocytes after hemin stimulation. The bars represent the SEM of the data from 3 samples per group. In D and E, *, P<0.05, **, P<0.01 compared to the hemin group. #, P<0.05 ## P<0.01 compared with the Gap19+hemin group. In the rest of the figures, *, P<0.05, **, P<0.01 compared to the control group. #, P<0.05, ##, P<0.01 compared to the hemin group.

Figure 6

Gap19 increases the activity of YAP in astrocytes exposed to ICH injury.(A) Immunofluorescence staining of astrocytes, microglia and neurons revealed that YAP was mainly expressed in astrocytes. (B, C) Gap19 was administered to astrocytes at the begining of hemin stimulation. Proteins were extracted 12 h after hemin stimulation, and the levels of Cx43, YAP and p-YAP were determined by WB analysis. Representative photos showing the levels of Cx43, YAP, p-YAP, and β-tubulin. (D) Immunofluorescence

showing the YAP nuclear translocation increased after treatment with Gap19 after hemin stimulation in astrocytes. (E, F) Quantitative WB analysis of YAP expression in the astrocyte cell cytoplasm and nucleus. The bars represent the SEM of the data from 3 samples per group. *, $P < 0.05$, **, $P < 0.01$ compared to the control group. #, $P < 0.05$, ##, $P < 0.01$ compared to the hemin group.
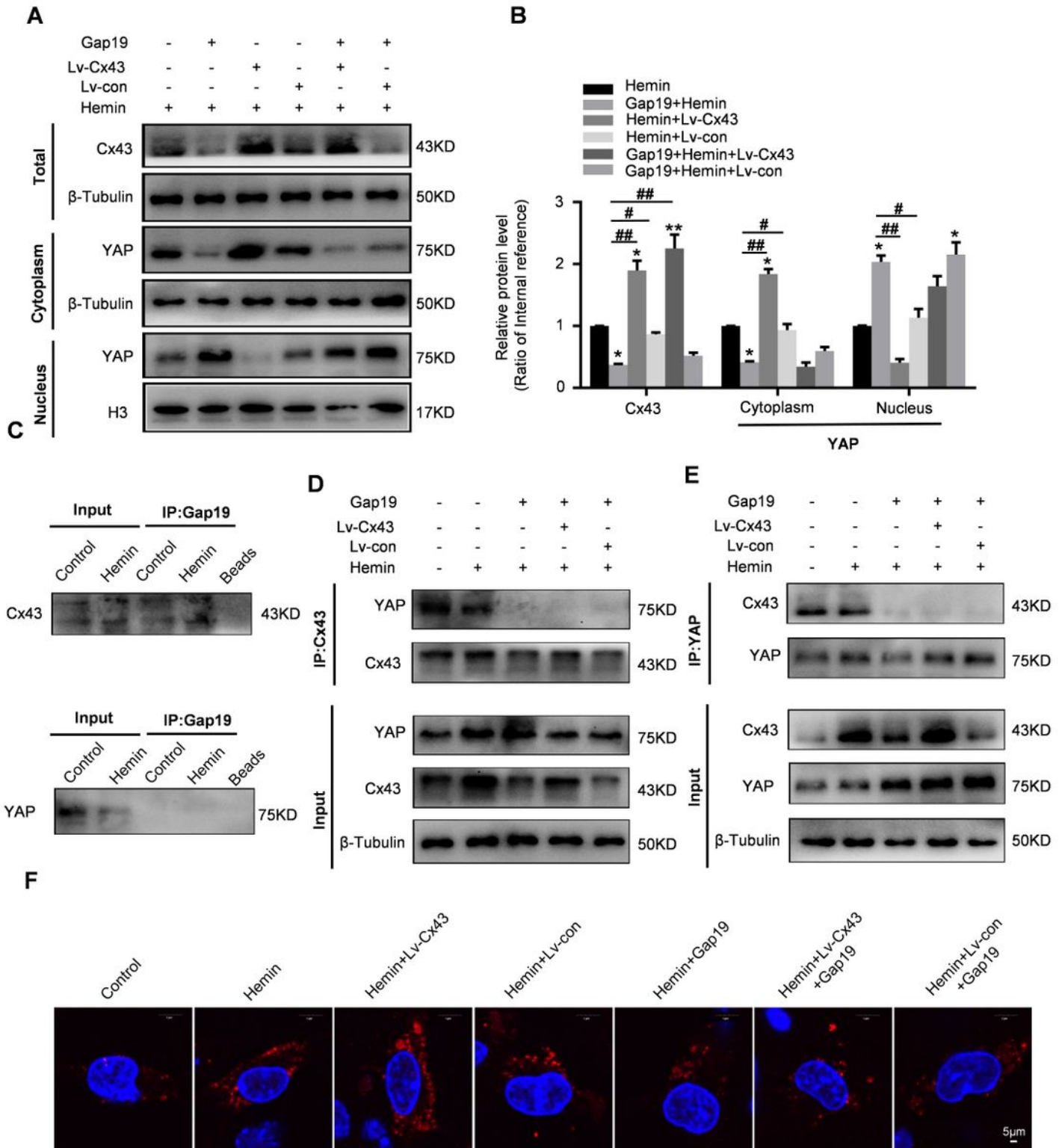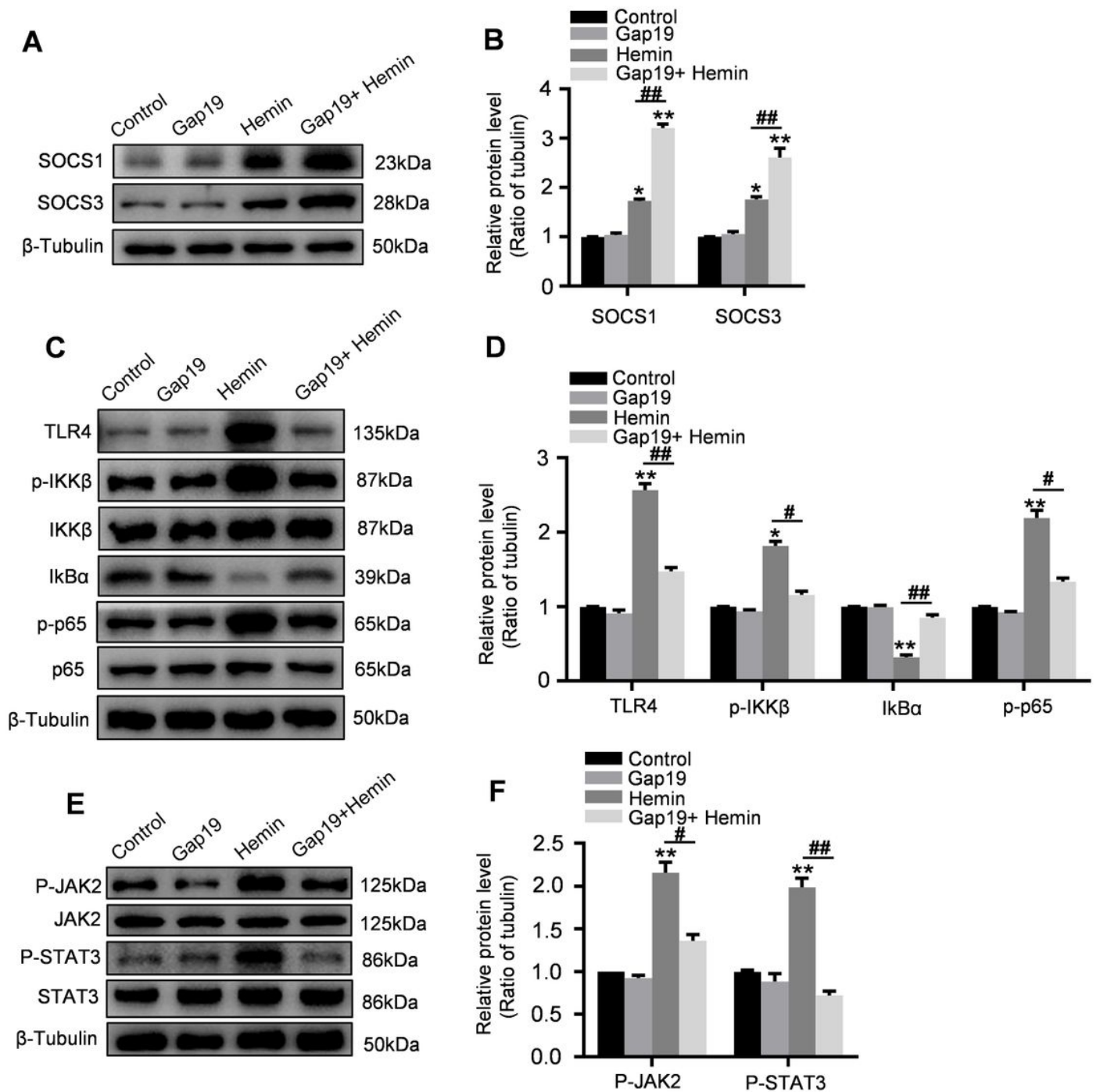

Figure 7

Gap19 regulates the physical association between astrocytic Cx43 and YAP in the cytoplasm after hemin stimulation.(A,B)Cx43 was overexpressed by lentiviral transfection,the levels of cytoplasmic/nuclearYAP was measured by WB in hemin-stimulated astrocytes.Quantitative analysis showing that Lv-Cx43 transfection decreased the nuclear YAP translocation after hemin stimulation.But Cx43 overexpression had no effects on YAP nuclear translocation after Gap19 treatment. (C) Coimmunoprecipitation experiments showing that Cx43 interacted with Gap19 but not YAP in hemin-stimulated astrocytes.(D, E) Coimmunoprecipitation experiments showing that YAP interacted with Cx43 and that Gap19 interfered with the binding of astrocytic Cx43 to YAP in the cytoplasm after hemin stimulation. (F) Representative images of the Duolink in situ PLA showing that there was a direct interaction between YAP and Cx43, that the effect was enhanced after Cx43 overexpression by Lv-Cx43, and that the interaction was weakened after Gap19 treatment. The bars represent the SEM of the data from 3 samples per group. *, P<0.05, ** P<0.01 compared to the hemin group. #, P<0.05, ##, P<0.01 compared with the Gap19+hemin group.
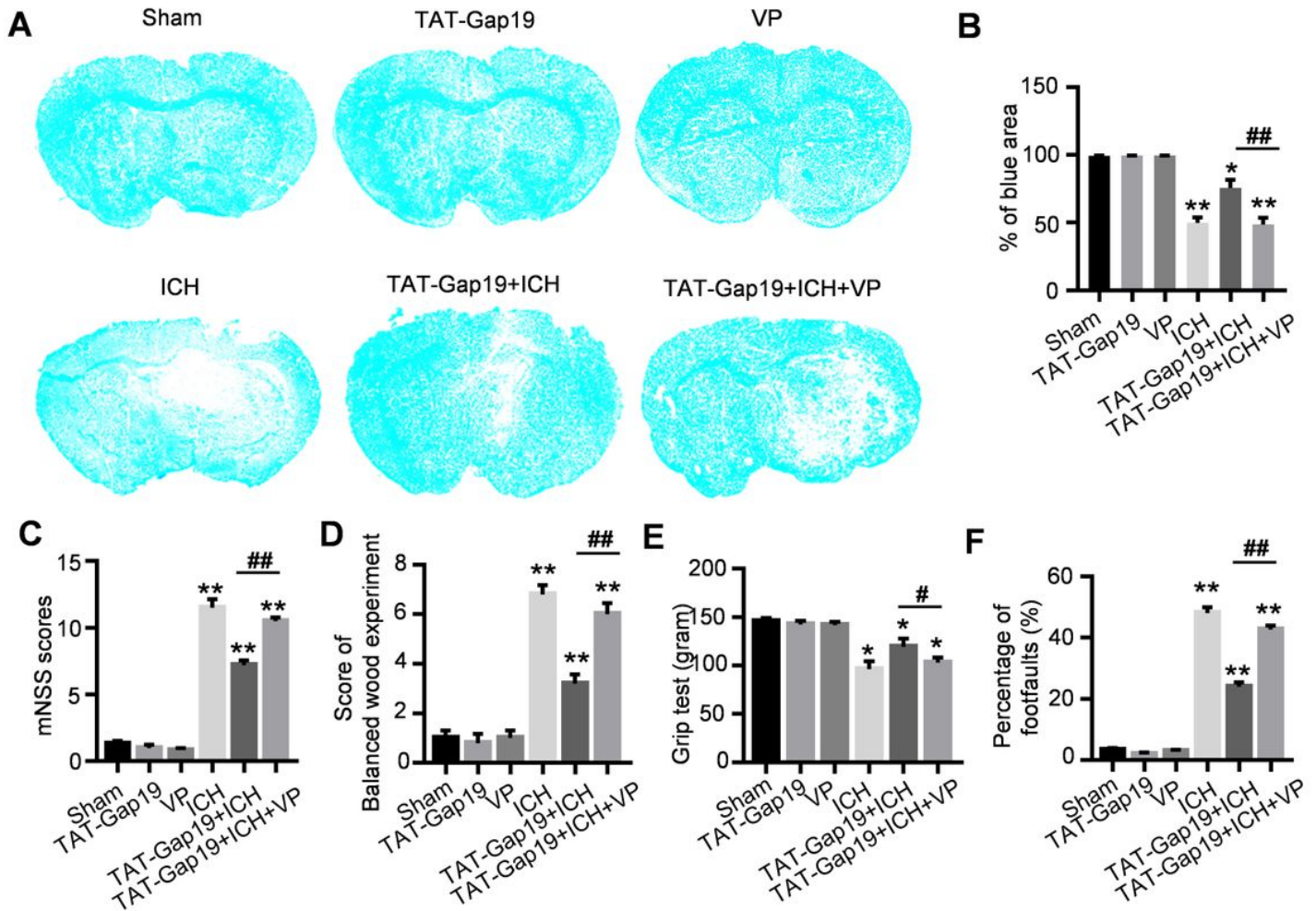
Figure 8

Gap19 regulates the Cx43-YAP-SOCS axis in reactive astrocytes after ICH injury.(A, B) Representative pictures showing the levels of SOCS1, SOCS3, and β-tubulin. (C, D) Representative pictures showing TLR4, p-IKKβ, IKKβ, IKBα, p65, p-p65, and β-tubulin levels. (E, F) Representative pictures show the levels of JAK2, p-JAK2, STAT3, p-STAT3, and β-tubulin. The bars represent the SEM of the data from 3 samples per group. *, P<0.05, ** P<0.01 compared to the hemin group. #, P<0.05, ##, P<0.01 compared with the Gap19+hemin group.
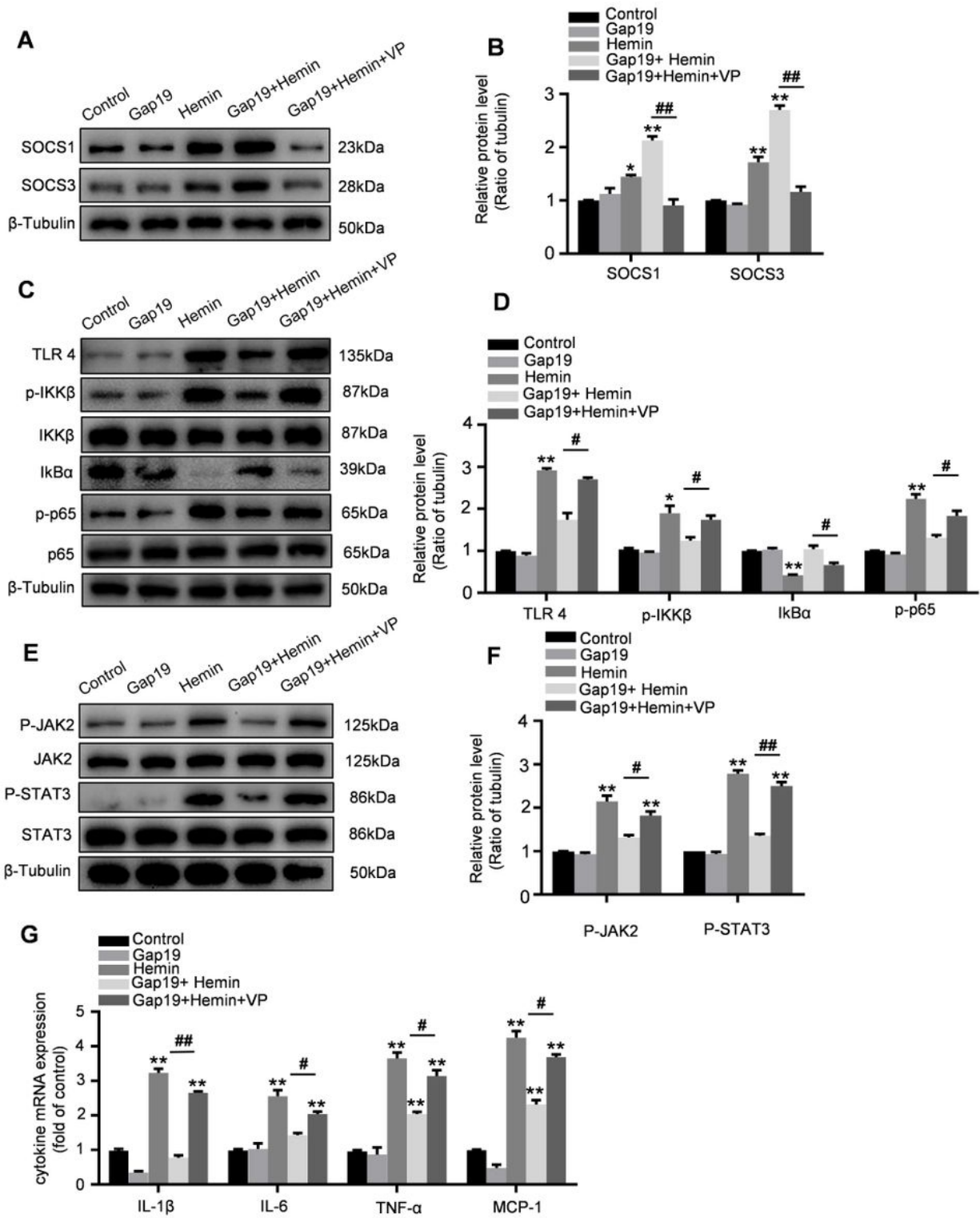
Figure 9

In vitro, the YAP inhibitor VP reverses the regulatory effect of Gap19 on the Cx43-YAP-SOCS axis (A, B) At the beginning of hemin stimulation, astrocytes were treated with the YAP inhibitor VP. WB analysis showed that VP suppressed the increase in SOCS1/SOCS3 levels induced by Gap19 treatment. (C, D) Representative photos showing the levels of TLR4, p-IKKβ, IKKβ, IKBα, p65, p-p65 and β-tubulin after treatment with the YAP inhibitor VP. (E, F) Representative photographs showing the levels of JAK2, p-

JAK2, STAT3, p-STAT3 and β-tubulin after treatment with the YAP inhibitor VP. (G) RT-PCR analysis of the transcriptional activities of IL-1β, IL-6, TNF-α and MCP1 in astrocytes after VP treatment. The bars represent the SEM of the data from 3 samples per group. *, P<0.05, ** P<0.01 compared to the hemin group. #, P<0.05, ##, P<0.01 compared with the Gap19+hemin group.

Figure 10

In vivo, the YAP inhibitor VP reverses the protective effect of Gap19 against the pathological process of ICH injury (A, B) Representative photos of LFB staining showing that the volume of cerebral hematoma in the TAT-Gap19+ICH+VP group was increased compared with that in the TAT-Gap19+ICH group and that VP reversed the protective effect of Gap19 against white matter damage after ICH. (C-F) The mNSSs, balance beam scores, foot fault rates, and forelimb grip strength of mice treated with the YAP inhibitor VP were evaluated and statistically analyzed. The represent the SEM of the data from 6 samples per group. *, P<0.05, ** P<0.01 compared to the sham group. #, P<0.05, ##, P<0.01 compared with the TAT-Gap19+ICH group.